Chemical Composition of CuInSe$_2$ Monograin Powders for Solar Cell Application

MARIT KAUK

TALLINN 2006

TALLINN UNIVERSITY OF TECHNOLOGY
Faculty of Chemistry and Materials Technology
Department of Materials Science
Chair of Semiconductor Materials Technology

Dissertation was accepted for the defence of the degree of Doctor of Philosophy in Natural and Exact Sciences on 27th of September, 2006

Supervisor: Leading Research Scientist Mare Altosaar, Faculty of Chemical and Materials Technology, Tallinn University of Technology

Opponents: Professor Dr.Sc. Vladimir Zlomanov,
Lomonosov Moscow State University

Senior Researcher Dr. Ants Lõhmus, University of Tartu

Defence: 7th of December, 2006 at 13.00
Lecture hall: VI-121
Tallinn University of Technology, Ehitajate tee 5, Tallinn

Declaration: Hereby I declare that this doctoral thesis, my original investigation and achievement, submitted for the doctoral degree at Tallinn University of Technology has not been submitted for any degree or examination.

Marit Kauk

Doktoritöö loodusteadustes

CuInSe$_2$ monoterapulbri koostise uurimine ja rakendus päikesepatareides

MARIT KAUK

TALLINN 2006

Table of Contents

List of publications

This thesis is based on the following appended papers, which are referred to in the text by their Roman numerals.

I **M. Kauk**, M. Altosaar, J. Raudoja, A. Jagomägi, M. Danilson, T. Varema, The performance of CuInSe$_2$ monograin layer solar cells with variable indium content, *accepted for publication in the Thin Solid Film, presented in the conference E-MRS 2006*

II K.Timmo, M.Altosaar, **M.Kauk**, J.Raudoja, E.Mellikov, CuInSe$_2$ monograin growth in the liquid phase of potassium iodide, *accepted for publication in the Thin Solid Film, presented in the conference E-MRS 2006*

III **M.Kauk**, K.Ernits, M. Grossberg, J.Krustok, T. Varema, M.Altosaar, E.Mellikov Chemical etching of CuInSe$_2$ absorber surface for monograin layer solar cell application, *Proceeding of the 20th European Photovoltaic Solar Energy Conference and Exhibition* (2006) 1811 - 1815

IV M. Altosaar, M. Danilson, **M. Kauk**, J. Krustok, E. Mellikov, J. Raudoja, K. Timmo, T.Varema, Further developments in CIS monograin layer solar cells technology, *Solar Energy Materials & Solar Cells* 87 (2005) 25-32

V **M. Kauk**, M. Altosaar, J. Raudoja, K. Timmo, M. Grossberg, T. Varema, E. Mellikov, Growth of CuInSe$_2$ monograin powders with different compositions, *Mater. Res. Soc. Symp. Proc.* Vol. 865, *Thin-Film Compound Semiconductor Photovoltaics*, 2005 F 14.27

VI **M.Kauk**, M.Altosaar, J.Raudoja, K.Timmo, M. Grossberg, T.Varema, K.Ernits, Tailoring the composition and properties of CuInSe$_2$ materials for solar cells application, *Proc. SPIE Vol. 5946, Optical Materials and Applications*, 2005, 224-229

VII M.Altosaar, A.Jagomägi, **M.Kauk**, M.Krunks, J.Krustok, E.Mellikov, J.Raudoja, T.Varema, Monograin layer solar cells. *Thin Solid Films* 431-432 (2003) 466-469.

VIII **M.Kauk**, M.Altosaar, J.Raudoja Influence of vacuum annealing on the composition of CuInSe$_2$, *Photovoltaic and Photoactive Materials - Properties, Technology and Applications, Kluwer academic publishers b.v.* Vol. 80, (2002) 337-339

IX M.Altosaar, **M.Kauk**, J.Raudoja, T.Varema, V.Geyer, "Verfahren zur Behandlung von Pulverkörner", Application for European Patent, EP1548845, 29.06.2005

X M.Altosaar, **M.Kauk**, J.Raudoja, T.Varema, V.Geyer, Method for treating powder particles, Application for International Patent, WO2005064691, 14.07.2005

Comments on my contributions

I   Part of the experimental work and major part of writing

II   Part of the experimental work (compositional analysis)

III   Part of the experimental work (chemical analysis, etching experiments) and major part of writing

IV   Part of the experimental work (compositional analysis)

V   Part of the experimental work (compositional analysis, electrical measurements) and major part of writing

VI   Part of the experimental work (compositional analysis, electrical measurements) and major part of writing

VII   Part of the experimental work

VIII   Part of the experimental work (compositional analysis) and writing with input from co-authors

List of abbreviations and symbols

Φ_b	barrier height of *p-n* junction
Δm	deviation from molecularity
Δs	deviation from stoichiometry
CBD	chemical bath deposition
CIS	$CuInSe_2$
EDS	energy dispersive spectroscopy
E_g	optical bandgap
EtOH	ethanol
j_{sc}	short circuit current density
I_{sc}	short circuit current
MGL	monograin layer
PL	photoluminescence
PU	polyurethane
QE	quantum efficiency
RT	room-temperature
SEM	scanning electron microscopy
V_{oc}	open circuit voltage
XPS	X-ray photoelectron spectroscopy
XRD	X-ray diffraction

INTRODUCTION

In today's climate of growing energy needs and increasing environmental concern, alternatives to the use of non-renewable and polluting fossil fuels have to be found and investigated. One such alternative source is solar energy. The major advantage of the photovoltaic systems is that they tap an almost inexhaustible resource that is free of charge and available everywhere in the world [1].

Solar cell technology dates to 1839 when French physicists Antoine-Cesar Becquerel and Alexandre Edmond Becquerel – father and son - observed that shining light on an electrode submerged in a conductive solution would create an electric current - the phenomenon called as photovoltaic effect. Over the following century, the conversion efficiencies of solar cells stayed below 1 %. The first cells yielding efficiencies of about 6 % were developed by Chapin *et al.* at Bell Labs in 1954 [1]. At that particular point in time, solar cells were made from semiconductor grade single crystalline silicon and were used as the power sources for space applications such as for satellites. The systems were very reliable, and cost was of little concern with regard to huge space program budgets.

Currently, the cost of photovoltaic systems is one of the main obstacles preventing production and application on a large scale. One approach to bring down the costs of solar cell production is to develop cheep technologies; one of them is the **monograin layer (MGL) solar cell technology.** The development of these new types of solar cells is promoted due to the possibility to make these cells almost unlimited areas.

This thesis is devoted to the absorber material properties in the field of development of MGL solar cells based on $CuInSe_2$ monograin powders. The thesis consists of four parts. Chapter 1 presents the structure of the CIS solar cell. Further, the known structural, electronic and optical properties of $CuInSe_2$ are compiled from literature data.

In Chapter 2, the used experimental technological approaches are described. Additionally, the design of the $CuInSe_2$ monograin layer solar cell and the procedures of its preparation are given. The methods used for the analysis of chemical and phase composition and for the investigation of properties of the absorber materials and developed devices on their bases are given.

The obtained experimental results and their discussion are presented in Chapter 3. The first part of this chapter contains the characteristics of CIS monograin powders grown in different flux materials. The deviation of materials from stoichiometry, crystal structure, morphology, electrical and optical properties depending on different process parameters are presented. The second part of this chapter presents the results of solar cells studies based on the grown $CuInSe_2$ monograin powders. The relationship between the solar cell efficiencies and the composition of $CuInSe_2$ powders is discussed. It is also demonstrated how the post-treatments in different atmospheres and chemical treatments of absorber material surface influence the solar cell parameters. Chapter 4 summarizes the main results obtained and presents conclusions of this work.

1. LITERATURE REVIEW AND AIM OF THE STUDY

1.1. CuInSe$_2$ based solar cells

CuInSe$_2$ as an absorber material in solar cells is mainly used in the form of thin films. Thin films are considered to have a large potential for the cost reductions of solar cells because of reduced material and energy consumption for their production. Conversion efficiencies between 12 and 15% have already been achieved for devices based on a pure CuInSe$_2$/CdS/ZnO heterojunction [2, 3, 4]. The bandgap of CIS can be continuously modified over a wide range (i.e. 1.0-1.65eV) by partial substitution of In with Ga or substitution of Se for S. [5]. Recent trends in CuInSe$_2$ research and development focus on these higher bandgap chalcopyrite alloys and record conversion efficiencies up to 19.5% [6] have been achieved until now.

At the same thin film technologies involve many drawbacks also, for example high cost of vacuum equipment in thin film production and uniform composition of films can hardly be achieved. The main advantage of the alternative powder based technology is the uniform homogeneous composition of grains in the whole patch. Since 2000, research in the Laboratory of Semiconductor Materials Technology of Tallinn University of Technology has been directed to the technologies of monograin powders of CuInSe$_2$ and monograin layer solar cells based on these powders [7].

1.2. Material properties of CuInSe$_2$

Hahn *et al.* first synthesized the ternary semiconductor CuInSe$_2$ in 1953 [8]. Since that time CIS has become a widely studied ternary material with applications in the areas of solar cells, non-linear optics and optical communications.

The electrical and optical properties of CIS materials are strongly dependent on their stoichiometric composition, defect chemistry and structure, which in turn are related to the growth parameters.

In this chapter, an introduction to structural and electronic properties of this material will be provided as a basis for the interpretation of the experimental results obtained.

1.2.1. Crystal structure

CuInSe$_2$ belongs to the family of I-III-VI$_2$ semiconductor materials that crystallize in the tetragonal chalcopyrite crystal structure. The tetragonal structure of CIS can be described as the stacking of two cubic zinc blende structures along the z-axis. The measured c/a ratio for the CIS is near 2. The lattice constant of CuInSe$_2$ has been widely studied and the early results by Spiess and co-workers [10] are in excellent agreement with the most recent measurements of bond lengths [11].
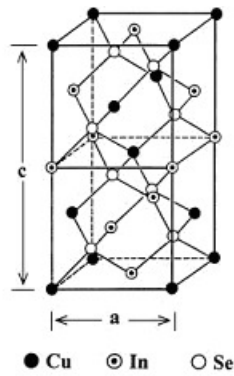
Fig. 1.1 Chalcopyrite unit cell for CuInSe₂ [9]

Typically measured values of lattice parameters of CuInSe$_2$ are a = 5.784 Å, c =11.616 Å. The unit cell of CuInSe$_2$ is shown in Fig. 1.1 [9].

1.2.2.   The phase relations in the Cu-In-Se system

The phase equilibrium of Cu-In-Se alloys has been of interest, providing basic understanding of material formation as a tool for fitting of parameters of technical applications based on the materials. Depending on the composition and the processing conditions, Cu-In-Se thin films possess a complex microstructure and contain a large variety of different phases. So far, however, it is not clear how the different phases influence the photovoltaic properties and how these phases evolve during material growth [12].
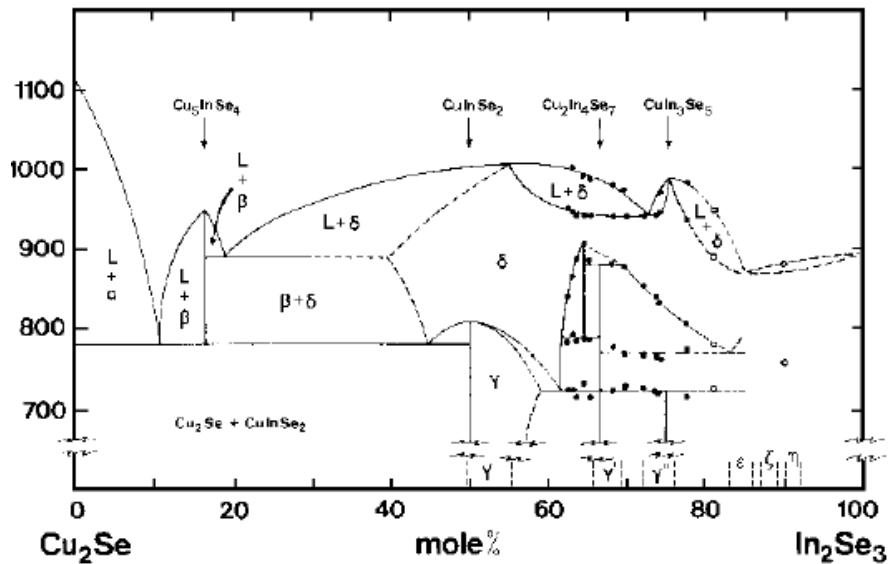
Fig. 1. 2 Cu₂Se-In₂Se₃ pseudobinary phase diagram [8]

The Cu_2Se–In_2Se_3 system has been investigated by several authors [8,13,14,15]. However, most of them consider the stoichiometric phase of $CuInSe_2$ as falling along the Cu_2Se-In_2Se_3 tie line on the ternary phase field of this system. One of more reliable pseudo-binary phase diagram that was determined by Fearheiley [8] is shown in Fig. 1.2.

According to the given phase diagram, various compounds (e.g. $Cu_2In_4Se_7$, $CuIn_3Se_5$, Cu_5InSe_4 and $CuInSe_2$) are likely to occur in this ternary system. At this diagram the chalcopyrite, single-phase $CuInSe_2$ extends from a stoichiometric composition of 50 mole% In_2Se_3 to the In-rich composition of about 55 mole % In_2Se_3. The corresponding Cu/In atomic ratio for this single-phase region lies between 1.0 and 0.82. If the Cu/In atomic ratios are greater than 1.0, the materials are expected to contain secondary phases of Cu_2Se and in contrast (Cu/In atomic ratio less than 0.82), the materials are expected to contain secondary phases of $Cu_2In_4Se_7$ and $CuIn_3Se_5$.
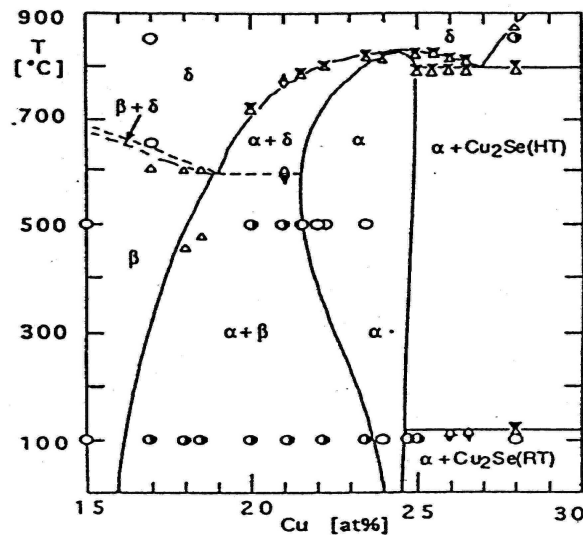
Figure 1.3 Cu_2Se-In_2Se_3 quasibinary phase diagram [15]

The phase diagram of $CuInSe_2$ was recently re-investigated by Haalboom et $al.$ [15] with a special focus on the temperature region between 20 - 900°C and the composition range of 15-30 at% Cu (Fig. 1.3). According to Haalboom et $al.$ the homogeneous α-phase is stable at composition range ≈ 24-24.5 at% Cu at room temperature. At higher temperatures, the existence range of single-phase $CuInSe_2$ is broadening to the In side and does not involve the stochiometric composition with 25% Cu as it was reported in [9, 13, 14]. The situation changes if indium is partially replaced in the crystal lattice with Ga [16] as well as if Na-doping is used. In both cases, the existence range of single phase of $CuInSe_2$ considerably widens [17, 18]. To summarize, the addition of Na prevents to some extent the formation of the β-phase in the system.

11

1.2.3. Optical properties

CuInSe$_2$ and related compounds have experienced considerable interest due to the extremely high absorption coefficient ($\alpha=10^5$ cm^{-1}), exhibited by these materials [19]. This high value of α implies that 99% of the incoming photons are absorbed within the first micrometer of the material. As a result, a layer with a thickness of only about 1µm is required to absorb effectively nearly all incoming photons.
Early measurements of the bandgap of single-crystalline CuInSe$_2$ exhibited nominal discrepancies [20, 21], suggesting a value in the range of 1.02 to 1.04 eV. Optical characterization of polycrystalline CuInSe$_2$ absorber films suitable for devices usually indicates to a significantly lower, approximately 0.9 eV, effective bandgap [22]. These variations in the optical properties of CuInSe$_2$ materials are a direct consequence of variations in the composition of various samples of single-crystalline crystals and thin films.

1.2.4. Defect composition of CuInSe$_2$ and electrical properties

The composition of CuInSe$_2$ could be described by two parameters, non-molecularity and non-stoichiometry, which have been defined by Groenink and Janse [23] as parameters Δm and Δs. These parameters determine the deviation from molecularity and stoichiometry, respectively:

$$\Delta m = \frac{[Cu]}{[In]} - 1 \tag{1}$$

$$\Delta s = \frac{2[Se]}{[Cu] + 3[In]} - 1 \tag{2}$$

The deviations of these parameters from zero indicate the following:
1. $\Delta m>0$ materials are Cu rich, probably containing the secondary phase of Cu$_{2-x}$Se
     $\Delta m<0$ materials are In rich, probably containing the secondary phase of In$_2$Se$_3$
2. $\Delta s >0$ materials are with excess of selenium
     $\Delta s <0$ materials are with selenium deficiency

The primary intrinsic defects in the CuInSe$_2$, which are also called native defects, include copper vacancies (V_{Cu}), copper-on-indium (Cu_{In}) antisites, indium-on-copper antisites (In_{Cu}), and selenium vacancies (V_{Se}). The former two are acceptor type defects, whereas the latter two give rise to donor-type defects. Depending upon the ratio of metal components, CuInSe$_2$ can be made either Cu-rich or In-rich. It is therefore possible to vary crucial electrical parameters by simple variation of the Cu/In atomic ratio and/or by changing the pressure of Se used during growth or

annealing [24, 25, 26]. Material is generally *p*-type, due to a large concentration of Cu_{In} defects. The performance of the solar cells that have Cu-rich absorber layers is usually low. This has been attributed to a high conductive Cu-Se separate phase that is located between the grain boundaries, and thereby shortens the *p-n* junction. The In-rich CuInSe$_2$ material, on the other hand, does not contain copper selenide separate phase. This type of material could be in either *n*- or *p*-type of conductivity. Usually, the In_{Cu} donor defects and the V_{Cu} acceptor defects are present at the same time in the material. As a result, conductivity of the layer is reduced due to the so-called *compensation* effect. The efficient self-doping ability of CuInSe$_2$ has been attributed to the exceptionally low formation energy of Cu vacancies and to the existence of a shallow Cu vacancy acceptor level [27].

However, so far, the problems of unambiguous identification of nonstoichiometric defects and establishment of the composition–property relationships are far from solution [27-31]. The authors of [32] have established the correlation between composition, type and concentration of nonstoichiometric defects, structure and properties of CuInSe$_2$ after equilibrium with various binary compounds CuSe, InSe, In$_2$Se$_3$ and Se. They proposed Cu_{In} substitution defects as most probable in the case of CuSe. An unexpected decrease in the charge carrier concentration (down to ~10^{16} cm^{-3}) and a simultaneous increase in the electron mobility (up to ~470 cm^2/V s) were observed when extrastoichiometric InSe (up to ~1.5–2 mol%) was introduced into CIS. They found that at higher Se concentration than 50.5 at.% the ordering of cation vacancies can occur. It was found that only the first portions of dopants produce electrical action, at higher concentrations the formation of electrically neutral complexes is probable.

In general, the conversion of *p*- to *n*-type corresponds to a strong decrease in the carrier concentration and conductivity [24]. In order to achieve high efficiency ZnO/CuInSe$_2$ heterojunction solar cell devices, a *p*-type absorber with an optimum carrier concentration of about 10^{16}-10^{17}cm^{-3} is required.

1.2.5. CuInSe$_2$ composition modification by post-treatments

1.2.5.1. Effect of thermal treatments

The electrical properties of the chalcopyrite phase have been reported to be critically dependent on the method of preparation and annealing treatments after fabrication.

In the equilibrium of gaseous and solid phases of CuInSe$_2$ the reaction of thermal dissociation of CuInSe$_2$ (3) offers a possibility to change the molecularity and the stoichiometry of CuInSe$_2$ by applying overpressure of In$_2$Se or Se$_2$ vapors [33]

$$2\ CuInSe_2 \rightarrow Cu_2Se\ (solid) + In_2Se\ (gas) + Se_2\ (gas) \qquad K_P = P_{In2Se}P_{Se2} \quad (3)$$
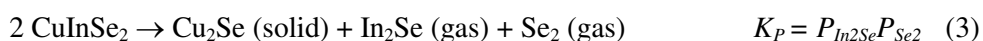
Several groups have reported an enhancement of the performance of CuInSe$_2$ devices after a post-deposition Se, S or vacuum annealing treatments. Since the freshly prepared (un-annealed) films have many defects such as voids, grain boundaries, dislocations, pin holes, etc., a mild heat treatment could be used for annealing out these defects. The annealing leads to stress relief and to the local structural rearrangements, resulting in recovery of stoichiometry in the films. The stress relief is caused by the reduction or removal of defects that results in the lowering of the charge carrier concentration and hence resistivity and capacitance [34]. Annealing in vacuum leads to the loss of selenium and recrystallization at temperatures higher than 673K [35, 36].

As was found in [37, 38, 39], temperature has a major influence on the defect structure of CIS. Therefore, heat treatment of different sequences is required. Se vapour treatment has been found to influence the bulk composition and structural properties, and the result is the increase of Se content [40]. Treatment in Se vapor shifts the PL band maximum to the higher values of energy. This is attributed to the filling of Se vacancies in the process of high Se pressure annealing [41].
Cu-poor n-type CIS becomes p-type by heating in Se overpressure and p-type CIS could be converted to n-type by thermal treatment in a Se low-pressure environment [42]. This effect is believed to originate from the selenium vacancy acting like a donor.

Although the direct bandgap of CuInSe$_2$ (1.04 eV) is quite well suited for fabrication of thin film solar cell devices, the values of bandgap of about 1.2 - 1.3eV are considered optimal for maximizing conversion efficiencies. Therefore, several technologies have been developed for the modification of composition (tailoring of bandgap) of CIS. There have been attempts to modify the bandgap of CuInSe$_2$ to better suit the solar spectrum. For example, CuIn(Se$_{1-x}$,S$_x$)$_2$ alloys have been produced by the systematic substitution of selenium (Se) with sulfur (S) atoms. CuInS$_2$ has a bandgap of about 1.55 eV and the bandgap of CuIn(Se$_{1-x}$,S$_x$)$_2$ ranges from 1.0 to 1.55 eV, depending on the concentration of S in the film. Systematic studies aimed to investigate sulphur diffusion into CIS and to produce materials with various Cu/In ratios have been carried out by [43, 44]. It was found that the bulk diffusion constants of S in Cu-rich and Cu-poor CIS were different by about two orders of magnitude and S inclusion is much more favourable in a Cu-rich material. It was found that a slight increase in surface roughness after sulfurization is revealed [45].
Recently it was found that it is desirable to have a larger bandgap region near the surface of the absorber where the junction is formed because this can potentially yield in devices with higher open circuit voltage values [45].
A widening of E_g will result in a reduced recombination rates. It is an advantage of CIS materials that E_g can be easily changed. Increased sulphur concentration will lower the position of valence band in the band scheme, leaving the conduction band location nearly unchanged. A lowered conduction band will reduce the hole

14

concentration and result in decreased recombination. This was confirmed experimentally by T. Walter *et al.* [46]. They found that the hole concentration decreases exponentially with the S/(Se+S) ratio.

1.2.5.2. Surface modification by chemical treatments

Controlled modifications of interface properties of a semiconductor are the key to improving the performance of a device. Although different research groups [48-58] have studied the influence of various chemical etchants for this purpose, detailed analytical investigations of surface composition studies of monograins to understand the effect of surface modifications and chemical changes occurring on the surface in the etching process have not been carried out.

In the studies [47,48] etching experiments in aqueous solutions with various pH and in the presence of oxidizing species of MnO_4^-, H_2SO_4 and H_2O_2 have been carried out. Authors used a thermodynamic approach to analyze the etching process of CIS. Manganese (VII) etching allowed either a continuous or a self-saturated etching, the hydrogen peroxide allowed stationary etching in the presence of EDTA. Peroxide as strong oxidizing agent, leaves a strongly oxidized metal-rich surface layer [49]. As a result, they were able to control the surface composition during etching in some conditions, but usually these etching processes could not be controlled.

Due to the segregation of Cu-Se binaries, it is necessary to remove these phases with strongly selective etchant that only attacks Cu-Se and does not harm the $CuInSe_2$. The only chemical etchants, which are presently known to fulfil this condition, are cyanide-containing solutions, such as potassium cyanide (KCN) [50, 51, 52, 53] and/or sodium cyanide (NaCN) [54, 55]. The cyanide etching solutions always contain potassium hydroxide (KOH) to avoid the formation of easily volatile and toxic hydrocyanic acid in the etching process. A KCN solution has been used to eliminate $Cu_{2-x}Se$ [52], $Cu_{2-x}S$ [53] impurities on the surface of Cu-rich CIS and $CuInS_2$, respectively their molecularity is changed drastically after the KCN treatment.

In the CBD process, the CdS layer is deposited in a solution containing NH_3. Treatment of CIS in a NH_3 solution was suggested to have an effect on the modification of the CIS surface [51, 52, 56, 57]. Ammonia etching leads to the complete removal of surface oxides [57, 58], to a significant increase of the surface Cu/In ratio, and to a removal of the initial surface inversion.

HCl etching is commonly used to remove CdS from $CdS/CuInSe_2$ devices. Therefore, influence of HCl treatment on CIS surface was investigated by Nelson *et al.* [56]. They found that after HCl etching the surfaces appeared to be unoxidized and Se rich. At the same time it does not affect the surface morphology significantly.

1.3. CuInSe$_2$ monograin powder growth

Isothermal recrystallization of II-VI and I-III-VI polycrystalline powders in the presence of liquid phase of a suitable solvent material (flux) in an amount sufficient for repelling the initial crystallites leads to the formation of semiconductor materials with single-crystalline grain structure and narrow-disperse granularity, so-called monograin powders. The driving force in this process is the difference of surface energy of crystals of different size. The growth of monocrystalline powder grains takes place at temperatures above the melting point of the used flux materials (much lower than the melting point of a semiconductor compound). Once the powder grains have the desired size, quenching stops the growth. Thereafter the fluxing agent is removed [59].

Research directed to the development of CIS monograin powder technology for solar cell application began at TUT in the Laboratory of Semiconductor Materials *from 1994* [60]. Already the first results indicated to a possibility of production of CIS monograin powders by recrystallization of polycrystalline powders in isothermal ampoules in the presence of liquid selenium [60].

Afterwards the recrystallization of polycrystalline powders was replaced with a similar process where the synthesis of the compound and the growth process were combined and proceeded in CuSe [61]. The used flux material has its specific impact on the properties of the grown material due to the doping of growing semiconductor (the matrix) crystals with constituent components of solvent at the level of solubility of these ones at growth temperature. From the technological point of view, the process of flux removal is also of great importance. Due to this, Se and CuSe, the flux materials difficult to remove, used before, have been now superseded by water-soluble potassium iodide.

The developed monograin powder technology [59- 63] appears to be relatively simple, inexpensive and convenient method to produce powder materials for solar cell applications. The main advantage of the powder crystals growth in a liquid flux is the uniform homogeneous composition of grains in the whole patch.

1.4. Motivation and objectives of the research

On the basis of literature review, the composition of CuInSe$_2$, as an absorber material of solar cells, is crucial since the most important output parameters of solar cell are influenced by deviations from molecularity and from stoichiometry. At the same time, the bulk composition and the surface composition of crystals can differ depending on deviation from molecularity and surface treatments. The doping of CuInSe$_2$ with Na (K) also influences the surface composition and defect structure (electrical and optical properties). The growth of monograin powders proceeds in a flux material (CuSe, KI) at elevated temperatures, this enables one to dope the growing materials and has a peculiar impact on the properties of grown crystals.

16

The main goal of the investigations basic for this dissertation was to determine regularities of the formation of CuInSe$_2$ monograin powders and optimal composition of device-quality CuInSe$_2$ monograin powders.

Specific objectives of this study were:

- to study the composition of CuInSe$_2$ monograin powders depending on the chemical nature of flux materials and on the Cu/In ratio in precursor materials;
- to determine the effect of composition of the monograin materials to structural, electrical and optical properties;
- to study the influence of thermal annealing in selenium and sulphur atmospheres and in vacuum on the bulk and surface chemical compositions and other properties of CuInSe$_2$ monograin powders;
- to study the effect of chemical treatments on the surface composition of CIS monograin powders;
- to develop the monograin layer solar cells in the use of CuInSe$_2$ materials with tailored volume and surface compositions and post-treated materials and to determine factors that are critical for the parameters of solar cells on bases of these materials.

2. EXPERIMENTAL PROCEDURES

The research performed and described in this thesis is focused 1) on the preparation of CuInSe$_2$ powder materials suitable for solar cell applications and 2) on the determination of regularities of different technological processes used for the formation of solar cells. The solar cell structure based on CuInSe$_2$ monograin powders will be presented, followed by a brief succession of steps of the cell fabrication process. The process of absorber material preparation will be described in more detail.

2.1. Monograin powder preparation

All powders used in this study were synthesized by Senior Researcher Jaan Raudoja and PhD. student Kristi Timmo.
A flow chart of processes in the monograin powder growth method for CIS is shown in Fig. 2.1. The CuInSe$_2$ compound was synthesized from high-purity elements (Cu, In, Se) in the liquid phase of a flux material in evacuated quartz ampoules.
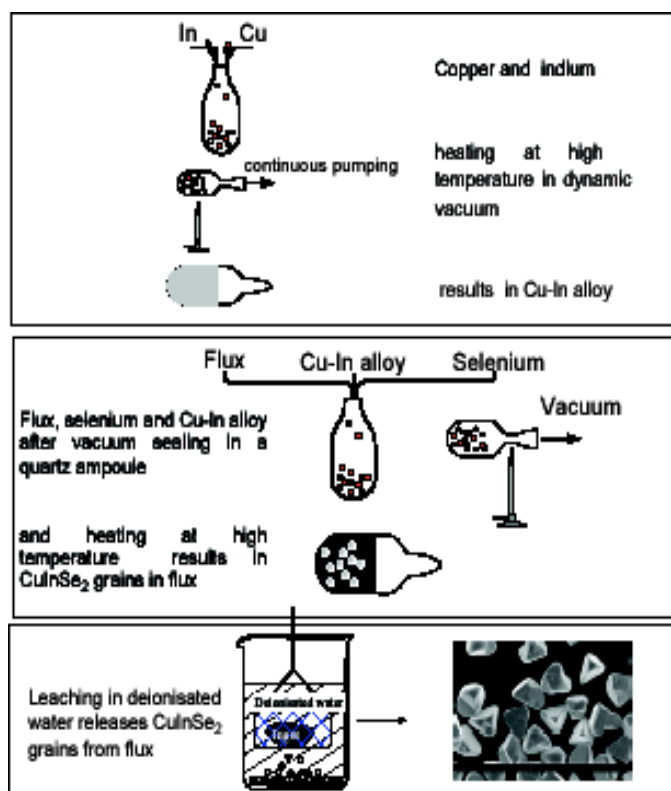
Fig.2.1 A schematic representation of the technology for CuInSe$_2$ monograin powder growth

In the first step, Cu-In alloys were synthesized in carbon-coated quartz tubes under dynamic vacuum (continuous pumping) at the temperature of 1070 K. After the thermal annealing process, ingots of Cu-In alloy were ground in a mortar.

The X-ray diffraction (XRD) spectra of the formed Cu-In alloys indicated to the formation of an alloy with a composition of $Cu_{11}In_9$ and separate metallic indium. According to Ref. [64, 65], the precursor metallic Cu-In alloys (with the indium composition of 47,62 at% - 60 at%) are identified as the mixtures of $Cu_{11}In_9$ compound and indium with the solidification temperature of 426 K. The presence of separate phase of metallic indium in In-rich precursors corresponds also to the equilibrium phase diagram [66]. Above the melting point of In, the equilibrium phases are liquid indium with Cu dissolved in it and solid Cu-In alloy. It has been observed by several investigators that $Cu_{11}In_9$ is the most commonly observed phase for Cu–In alloys [67].

Next, the ground Cu-In alloy and elemental Se were mixed with a desired amount of flux. The amount of components for $CuInSe_2$ syntheses and the amount of flux were nearly equal to provide the volume of liquid phases enough for the monograin growth. The melting temperature of the used flux material limits the minimum growth temperature and the temperature of the phase transition of CIS (1083K) limits the maximum growth temperature. Samples were sealed into evacuated quartz ampoules, annealed isothermally at various temperatures and quenched to room temperature. The used flux was removed by deionized water (KI) or in 10% KCN aqueous solution (CuSe-Se). Finally, the well-dried powders were sieved to narrow fractions from 20μm to 112μm. More detailed description of the procedure of materials preparation is presented in papers [II, IV, V, VII].

2.2. Post-treatments of CuInSe₂ monograin powders

All CIS powders used as absorber materials in monograin layer solar cells were post-treated in various atmospheres. Technological parameters of thermal post-treatments are briefly summarized in Table 2.1.

Table 2.1. Parameters of thermal treatments of CIS monograin powders

Atmosphere of the treatment	Temperature, K/ vapour pressure, Torr	Duration	Results published
Vacuum, 10^{-2} Torr	473–873	5-120 min.	VI, VII, VIII
Se vapour	803/ 0.1 to 50 Torr	2-40 h	IV, VI
S vapour	683–843/ 0.01 –10 Torr	2-66 h	I, IV, VI

The interface of CIS/CdS heterojunction is the key factor of further improvements of solar cell performance; therefore, various surface treatments of CIS were made prior to the deposition of the CdS buffer layer. The choice of chemical reagents for

surface modification of monograin powder crystals in the chemical etching process was based on the following considerations (see also Table 2.2):

- KCN solutions are well-known and used everywhere as selective etchants for copper binary phases and for elemental S and Se [68,69];
- HCl and NH_3 treatments are used as processes of CIS solar cells for removal of surface oxides [49,70] and In-rich OVC layer [71];
- Etching in KOH-in-ethanol solution is an essential step in the monograin layer technology.

Table.2.2 The details of the ecthants used in this study

Chemical	Concentration
KOH-etOH	10g KOH + 100g C_2H_5OH
HCl	Concentrated (37%)
NH_4OH	1M
KCN	10% KCN+ 0.5% KOH

The powders etched in different etchants were later used as absorber materials in monograin layer solar cells and the influence of chemical etching to their output characteristics was studied. More detailed description of the results obtained can be found in paper [III].

2.3.   Characterization Techniques

2.3.1.   Material characterization

In this study, a wide variety of characterization techniques was used to evaluate the material quality.

- *Composition*

The bulk composition of powders was determined polarographically and by energy-dispersive X-ray analysis (EDS). Polarographic analyses were made with Metrhom polarograph, which consisted of two parts: 746 VA Trace Analyzer and 747 VA Stand. EDS analyses were done by researcher O. Volobujeva using Röntex EDS detector (LEO SUPRA 35). The surface composition of chemically etched powder crystals was determined by XPS (in Stuttgart University, Germany).

- *Morphology and phase composition*

The surface morphology and phase composition of the developed materials were examined by the high-resolution scanning electron microscopy (LEO SUPRA 35) and XRD, respectively. O. Volobujeva, Department of Materials Science, Tallinn University of Technology, operated the SEM. XRD patterns shown in the present thesis were acquired on Bruker AXS D5005 diffractometer with the

monochromatic Cu Kα radiation, analyzed by Researcher-Professor M. Krunks (TUT).

- *Optical and electrical measurements*

Optical parameters, phase composition and defect structure were characterized by photoluminescence (PL) spectroscopy. For the photoluminescence (PL) measurements, the closed-cycle He cryostat (T = 9 - 300 K) and the He-Cd laser were used. The PL signal was detected using a standard lock-in technique, computer-controlled SPM-2 grating monochromator (f = 40 cm) and an InGaAs detector. The signal detected was corrected in conformity with the grating efficiency and detector sensitivity spectra.

The electrical resistance of the grain was determined by pressing the grain between two indium contacts. The ohmic behaviour of contacts was proven by the linearity of *I-V* curves. The conductivity type was determined by the hot-probe method.

2.3.2.   Device characterization

Completed solar cell structures were characterized by dark and light current-voltage (*I-V*) and quantum efficiency (QE) measurements. Measurements were performed using an AUTOLAB PGSTAT 30 set-up. From the results of light current-voltage measurements under standard test conditions (AM 1.5, 1000 W/m^2, 25°C) the most important solar cell parameters, efficiency η, short circuit current density J_{sc}, open circuit voltage V_{oc} and fill factor *FF* were extracted.

The efficiency of solar cell is the most important characteristic of a solar cell, given by Eq. (4)

$$\eta = \frac{J_{sc} \cdot V_{oc} \cdot FF}{P_s} \tag{4}$$

where P_s is power of the standard illumination of AM1.5 (100 mW/cm^2).

The fill factor (FF) is often used to characterize the quality of a solar cell junction, calculated by Eq. (5)

$$FF = \frac{J_m \cdot V_m}{J_{sc} \cdot V_{oc}} \tag{5}$$

where J_m is current density at maximum power output and V_m is voltage at maximum power output.

Spectral response measurements were performed using a computer-controlled SPM-2 monochromator and a 100W halogen lamp. For bias-dependent measurements, the Autolab PGSTAT-30 together with a lock-in amplifier were used. All temperature-dependent measurements were made in a closed-cycle He cryostat (*T*= 10 - 300 K).

3. RESULTS AND DISCUSSION

3.1. Properties of as-grown powders

As it was described in section 2.1, $CuInSe_2$ powder materials were synthesized from Cu-In alloy and Se in liquid phase of molten fluxes. Two different fluxes – CuSe-Se and potassium iodide (KI) - were used. CuSe is a suitable flux material due to its consistent elements that are inherent to the CIS compound and thereby the doping of CIS with foreign dopants is avoided. CuSe has relatively low melting temperature (673 K). Addition of extra selenium into the CuSe flux is necessary because it holds back the thermal dissociation of CuSe. After growth, the dissolution of CuSe-Se flux was realized by leaching with 10% KCN solution. A major technological advantage of the usage of KI as a flux material is the possibility of removing it after the growth process very easily by a simple dissolution process in distillated or DI water. The other advantage is the possibility to change In content in the grown powders by changing the Cu/In ratio in precursor alloys. The drawback of the usage of KI is possible contamination of CIS crystals with potassium and iodine at the level of solubility of them in CIS at growth temperature.

3.1.1. Composition of $CuInSe_2$ powders grown in CuSe-Se flux

During the first stage of the PhD. research, CuSe-Se flux was used as a flux for growth of $CuInSe_2$ monograin powders. According to the papers concerning the formation of $CuInSe_2$ and the phase diagram of Cu-Se [72], no other solid phases exist in the system used, except for $CuInSe_2$ at temperatures higher than 803K. It has been demonstrated that liquid binary Cu-Se phases promote the growth of large $CuInSe_2$ grains [61] and Cu-Se binaries have already been used for the solution growth of bulk $CuInSe_2$ crystals [73]. The amount of components for $CuInSe_2$ and the amount of flux were found to be nearly equal for providing the amount of liquid phase for the monograin growth.

In order to investigate the influence of several growth parameters on the chemical and phase composition and properties of CIS monograin powders, the following technological parameters were varied:
- The ratio of Cu/In in metal precursor;
- The ratio of CIS/flux;
- The growth temperature

The deviations from molecularity (Δm) and from stoichiometry (Δs) were calculated from polarographic analysis data, presented in Fig. 3.1.

All the obtained results show that there is possibility to gain both - copper side and indium side deviations from molecularity of composition of $CuInSe_2$ crystals grown in the CuSe-Se flux. The molecularity Δm was found to be dependent on selenium content in the CuSe-Se flux (see Fig 3.1.a). In powders grown without extra Se in the CuSe, Δm had negative values and Δm increased with increasing

extra Se content in the CuSe-Se up to 5 %. Over 5% of extra Se in flux, the Δm had positive values. The materials grown at 1003K had more In-rich compositions as compared to the materials grown at 803K. The results are in good correspondence with the phase diagram of Cu_2Se-In_2Se_3 (see Fig. 1.3). The single-phase region of $CuInSe_2$ has a little crook to the Cu-rich side at higher temperatures. In comparison with the phase equilibrium of $CuInSe_2$-Cu_2Se, compositions of $CuInSe_2$ are shifted to more Cu-rich side in equilibrium with CuSe-Se liquid phase and the shift depends on the Se content in the system. The scattering of polarographic analysis data is rather high. It is possible that the cooling rate of different samples can vary and the high temperature equilibrium of phases is frozen in at different levels or some amount of CuSe flux could remain unremoved from the inside of crystals of CIS before dissolution of probes for polarographic analysis.
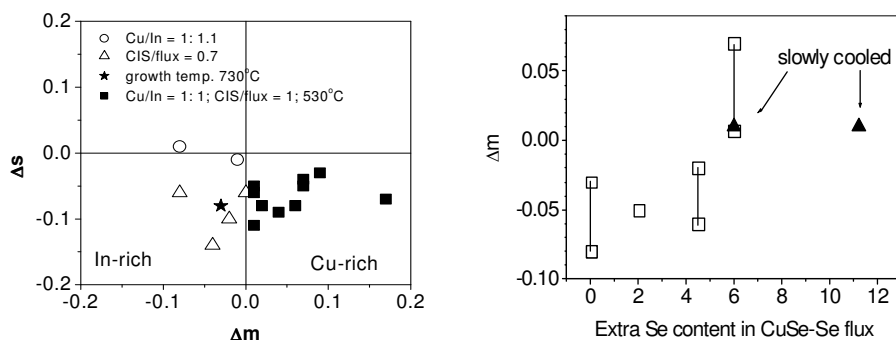
Fig. 3.1 Deviations from molecularity and stoichiometry in CuInSe$_2$ monograin powders grown in CuSe flux. Fig. 3.1a Molecularity dependent on selenium content in the CuSe-Se flux

All of these as-grown materials were *p*-type but highly conductive. Grain resistances were in the range of 10^2- 10^3 Ω and they were dependent on Se content in the CuSe-Se flux. The high concentrations of carriers in grown powders made the materials not suitable for solar cell application.

As it was not possible to grow CIS powders with more In-rich compositions in CuSe-Se flux, it was necessary to find another flux material to satisfy In-rich composition criteria for solar cell absorber material. It is well known that alkaline halogenides are water-soluble and that iodine has low solubility in CIS materials (agent of chemical transport reaction) [74]. It was also known that Na and K as dopants in CIS have positive impact on the absorber material properties [75,76,77]. These considerations led to the idea to use KI as a flux material for CuInSe$_2$ monograin powder growth.

3.1.2.   Composition of powders grown in potassium iodide flux

Potassium iodide is a suitable flux compound for several reasons:
- The melting point of KI is lower (953 K- 959 K) than the temperature of phase transition of $CuInSe_2$
- KI is water soluble (no need to use cyanide solutions)
- The solubility of CIS in KI is 0.17 ± 0.05 wt. % [78] (it is 50 times less than in the CuSe-Se flux)
- Potassium (K) as a dopant promotes the formation of materials with *p*-type conductivity [79].
- KI flux does not contain base material components. Thereby, it allows for precise control of the Cu/In ratio in $CuInSe_2$ monograin powders.

More details about growth parameters of CIS in the KI flux are presented in [II]. In order to grow $CuInSe_2$ MGP-s with different compositions, Cu-In alloys with different Cu/In concentration ratios (0.5- 1.1) as precursor materials were prepared. The results of the research of modifying CIS monograin powder growth in KI flux in the single-phase region of CIS phase diagram are described in papers [I, V, VI].

The optimal Cu content in thin film CIS absorbers for solar cells varies from 22 to 24 at. % Cu. This composition lies within the single-phase region of α-phase at the used growth temperature. However, during the cooling down to the room temperature material composition enters the two-phase ($\alpha+\beta$) region in the equilibrium phase diagram (see Fig. 1.3). The situation described above could lead to the formation of multiphase product at the slow cooling process of materials. Fortunately, it is known that Na (K) incorporation into the CIS widens the existence range of the α-($CuInSe_2$) phase in the phase diagram. Table 3.1 shows the Cu/In concentration ratios of Cu-In alloys, deviation from molecularity and deviation from stochiometry, as calculated from the polarographic analysis data of grown powders and the conductivity type of developed powders.

Table 3.1. [Cu]/[In] in Cu-In alloy, powder analysis data, Δm and Δs (calculated from polarographic analysis data) and conductivity type of CIS monograin powders

[Cu]/[In] in Cu-In alloy	Cu, at%	In, at%	Se, at%	Δm	Δs	Conductivity type
1.1	25.8	24.9	49.4	0.04	-0.02	*p*
1	24.1	25.6	50.4	-0.06	0.00	*p*
0.92	23.7	25.6	50.7	-0.07	0.01	*p*
0.83	22.7	26.2	51.0	-0.13	0.01	*p*
0.71	20.6	27.1	52.3	-0.24	0.03	*p*
0.66	19.1	29.0	51.9	-0.34	-0.02	*p, n*
0.59	18.0	30.3	51.6	-0.40	-0.05	*n*
0.5	15.7	33.1	51.2	-0.52	-0.11	*n*

The Cu/In concentration ratios of the grown powders (determined polarographically) versus those of the Cu-In alloys are shown in Fig. 3.2. In the case of In-rich precursor alloys ([Cu]/[In]<1), Cu/In ratios in the grown powders are nearly equal to the Cu/In ratios of initial Cu-In alloys (or slightly less indium-rich). Powder materials from the Cu-rich ([Cu]/[In] ≥1) initial compositions "have lost" some amount of copper. This indicates that material composition has entered the multiphase region of the phase diagram. Additionally, we determined Cu, In, and Se concentrations in the leaching solutions and found that relative Cu concentrations in leaching solutions were in the range of 25-26 at%, while the corresponding In concentrations were 21-23 at%.
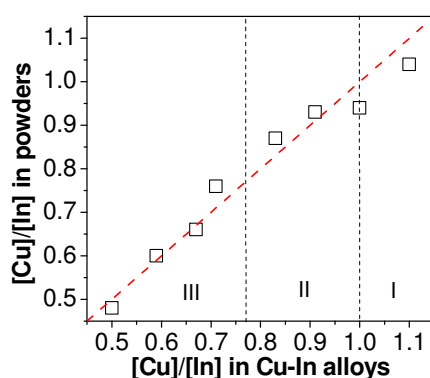
Fig. 3.2. Composition ratio of Cu/In in powders plotted as a function of Cu/In ratio in the Cu-In alloys. The dashed line marks the equal values of Cu/In ratios.

The EDS analysis of single powder grains showed that the materials with Cu/In≥0.77 consisted of the crystals with uniform composition. At the same time, the powder with Cu/In=0.67 consisted of crystals with two different compositions: with Cu/In = 0.92 and with Cu/In=0.66. Thus, it can be confirmed that a multiphase solid material was formed.

The obtained results suggest that the Cu/In composition can be well controlled by the Cu/In ratio in the CuIn alloy.

The selenium concentration of the synthesized powders, determined polarographically and by EDS, as the function of the Cu/In ratio, is presented in Fig.3.3. Selenium content in the powders increases with decreasing molecularity and changes from 49 at% up to about 54 at%.
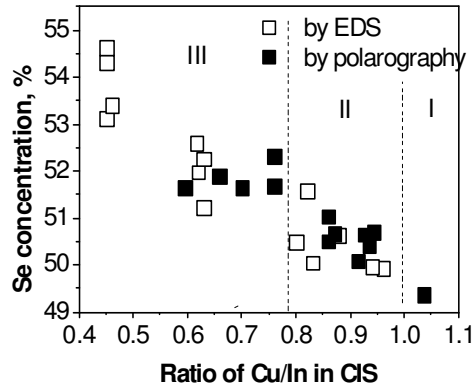
Fig. 3.3. Selenium content in powder as function of Cu/In in CIS

Figs. 3.2 and 3.3 indicate to three regions in Cu/In ratios. Each region is characterized by different crystal growth equilibrium and with different compositions of powders. The approximate borders of those regions are marked with dashed lines. The border of II/III region coincides with the changes of the type of conductivity of as grown powder crystals. Single α-phase $CuInSe_2$ monograin powders could be produced in the II region (0.77<Cu/In<1).

3.1.3. Structural properties

The results of the XRD study of powders with the Cu/In ratio between 0.5-1.1 are presented in paper [I].
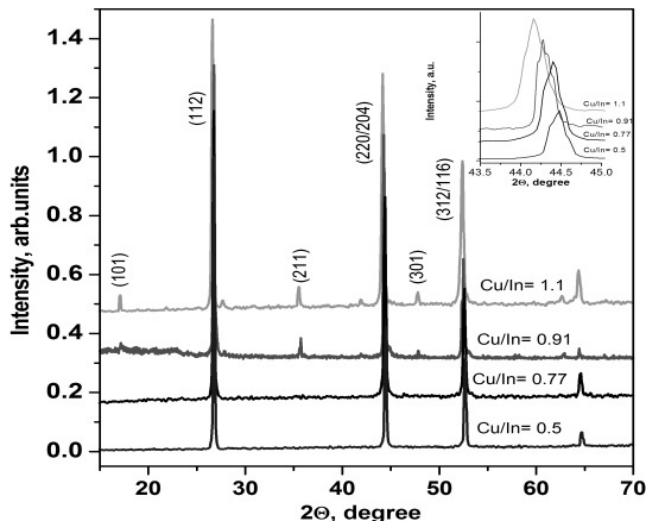
Fig. 3.4. XRD patterns of monograin powders with different Cu/In ratios

XRD patterns of stoichiometric or slightly In-rich as-grown powders showed very sharp reflections, spectra revealed the presence of a single phase, corresponding to the $CuInSe_2$ chalcopyrite compound. In XRD spectra for materials with the Cu/In ratio less than 0.77, the (101), (211), (301) reflection peaks disappeared. Additionally, the reflection peaks (220/204) and (312/116) were shifted to the right side. Similar changes in XRD spectra are attributed in literature to appearance of a new phase - $Cu_2In_4Se_7$ - in the system [80]. Only reflections typical of CIS appeared in the XRD spectra of Cu-rich materials, there were no reflections of possible additional phases. This confirms that the single phase $CuInSe_2$ chalcopyrite material was formed in the Cu-rich growth process or the content of CuSe ($Cu_{2-x}Se$) was below the XRD detection sensitivity.

3.1.4.   Morphology of grown crystals

Our SEM studies revealed that flux material and Cu/In ratio in $CuInSe_2$ crystals has a substantial effect on the crystal size and surface morphology.
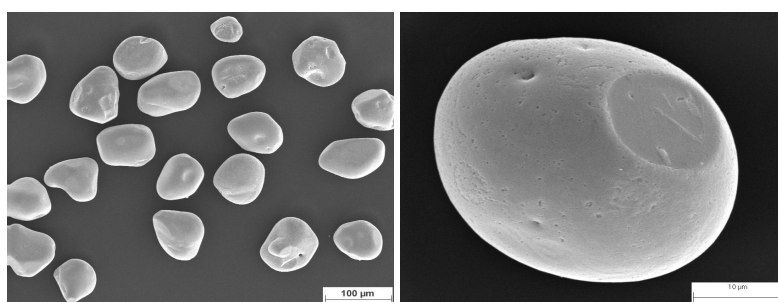
Fig. 3.5 Monograin powder grown from CuSe-Se flux
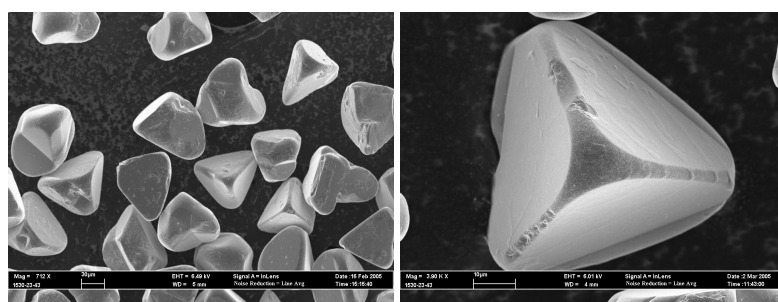
Fig. 3.6 Monograin powder grown from KI flux

Morphology of monograins drastically changes depending on the flux material. SEM studies showed that monograins grown in CuSe flux are orbicular, but the use of KI flux resulted in tetrahedral shape of grains. It could be explained with different solubility of CIS in CuSe and KI. The solubility of $CuInSe_2$ in molten fluxes was determined by the weight loss method, the description of this method and the results are presented in paper [II].
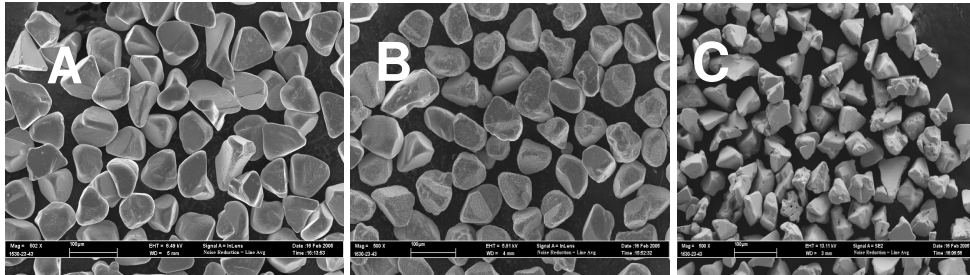
**Fig. 3.7. SEM micrographs of CuInSe₂ monograin powders with different Cu/In ratios
A) Cu/In = 1.1:1; B) Cu/In = 1:1.1; C) Cu/In = 1:1.5**

SEM studies confirm an increase in grain size by increasing the Cu/In ratio in powders. The obtained results indicate that the growth of CIS under slightly In-rich or stoichiometric conditions leads to larger grains. The mechanism of sintering of powder crystals is revealed more clearly for highly In-rich powders.

3.1.5.   PL study of CuInSe₂ powders

The shape of PL spectra is a valuable tool to verify deviations from the stoichiometric composition. Fig. 3.8 shows the PL spectrum of a Cu-rich CIS grown in the CuSe-Se flux. The PL spectrum has a narrow symmetrical band with the peak maximum at 0.973 eV and another band at 1.04 eV that corresponds to the bandgap of $CuInSe_2$.
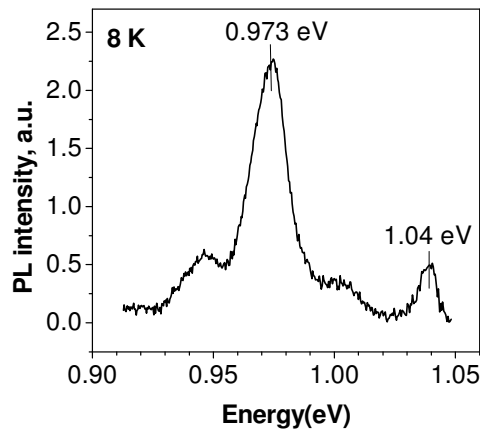
Fig. 3.8 PL spectra of Cu-rich CuInSe₂ grown in CuSe-Se flux
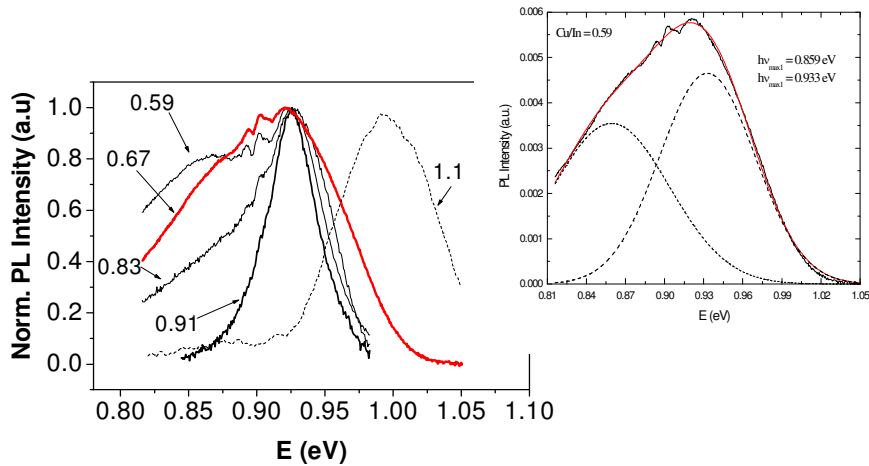
Fig. 3.9 PL spectra of Cu-rich, near stoichiometric and In-rich CuInSe$_2$ at 9K. The Cu/In ratio of precursor Cu-In alloys is shown numerically.

Fig. 3.9 shows the PL spectra of CIS powders with different indium contents. The change of the In content in CIS influences the shape of the PL spectrum and the positions of the peaks maxima in spectra. A broad asymmetric band characterizes the typical PL spectrum of In-rich CIS with the maximum around 0.93 eV. The PL spectra of In-rich samples (Cu/In<0.83) exhibit two broad bands with peak positions at ~0.86 and 0.93eV. The broad band at ~ 0.86 eV is probably related to the recombination through deep intrinsic defect levels (~245 meV) that are caused by indium interstitials (In$_i$) or In$_{Cu}$ [81]. The relative intensity of the latter band increases with the increasing indium content, which seems to be a prerequisite for the creation of corresponding defects. The wide PL peak at about 0.99 eV dominates the PL spectra of Cu-rich powders.

3.1.6.   Electrical resistance and conductivity type

According to literature review, CIS having *p*-type charge transport mechanism is used as an absorber in solar cells. The type of electrical conduction in CIS depends on its elemental composition [82]. Therefore, it is essential to attain the skill and ability to control the type of conduction in CIS powder crystals. Fig. 3.10 shows the electrical resistance of as-grown CuInSe$_2$ grains as the function of Cu/In molar ratio of precursor Cu-In alloys. All the measured grains were in sizes of 112-150μm.
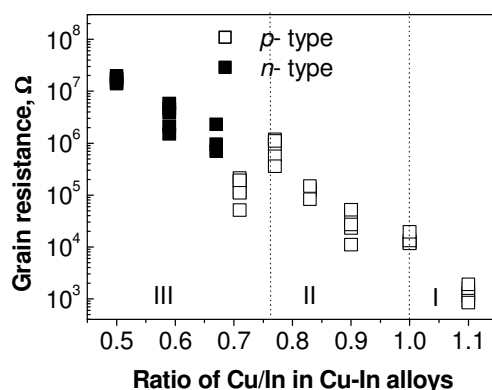
Fig. 3.10. Grain resistance depending on the Cu/In ratio in the material (measured grain sizes within 112-150 μm)

The data of resistance measurement for grains with compositions corresponding to the *n*-type region are represented by solid squares, while the *p*-type ones are shown as open squares. As the Cu/In ratio increases from 0.5 to 1.1, the grain resistance decreases from 2×10^7 to 8×10^2 Ω. The change of conductivity type occurs in the region of the Cu/In ratio values of 0.67-0.71. Within this region, the materials consist of crystals with both different types of conductivity. According to EDS analysis, materials consist of crystals with different compositions: with Cu/In=0.92 and Cu/In=0.66. Based on the results of EDS and grain resistance, we can conclude that crystal growth at this initial composition takes place in multiphase conditions. In that region materials selenium content of materials is rather high (about 52 at%).

3.2. Modification of composition of monograin powders

In most cases, as-grown powders need post-treatment in different gaseous ambients to improve properties for using powders as absorber materials. For this purpose, selenization and/or sulfurization were used. Se vapour treatment has been found to influence the bulk composition [83]. Sulfurization of the powders is formed in CuInSe$_2$ crystal surface region with a higher bandgap that is a precondition for the development of devices with higher open circuit voltage (V_{oc}).
Different chemical treatments of surfaces of CuInSe$_2$ powder crystals were used to improve the interface properties of CuInSe$_2$/CdS heterojunction.

Thermal treatment in vacuum
CuInSe$_2$ powder materials were annealed in dynamic vacuum (10^{-2} Torr) (continuous pumping) at different temperatures and process durations. The EDS results for the annealed materials did not show any remarkable changes in molecularity but indicated to the loss of selenium already after 5 min annealing at 473K, making it possible to generate selenium vacancies V_{Se} that act as donors in

30

p-type CuInSe$_2$. As it was found [VIII], the grain resistivity increases during a 15min vacuum annealing process with the increase of annealing temperature up to 673K. At higher annealing temperatures grain resistivity decreases. We suppose that at higher temperatures than 673-723K, besides the loss of selenium, the thermal dissociation of the ternary compound CuInSe$_2$ becomes remarkable, resulting in the loss of In$_2$Se [84].
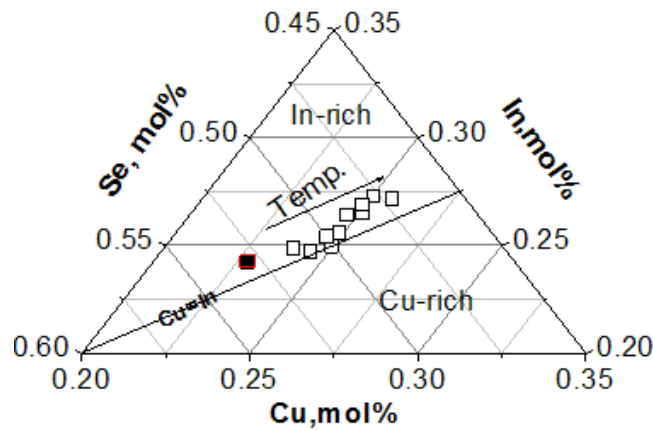
Fig. 3.11 Compositions of vacuum annealed CuInSe$_2$ powders plotted in the ternary phase diagram. Filled square indicates the as-grown powder composition. Temperature was varied from 373- 773 K , annealing time was constantly 15 minutes.

Thermal treatment in Se vapor

In the selenization studies, different selenium vapour pressures (0.1 to 50 Torr) were applied to the CuInSe$_2$ monograin powder (Δm<0) in two-zone quartz ampoules (803K, *t*=17 h). The ampoules were placed into a two-zone tube furnace, where the temperature of both zones were controlled and regulated precisely. In such an arrangement, Se vapour pressure was determined and controlled by the lowest temperature in the system.

The results of the polarographic analyses showed (Fig. 3.12) that initially slight In-rich composition of the material (Δm<0) (shown in the figure as "as-grown") became slightly Cu-rich (Δm>0) at lower Se pressures than 5 Torr. The positive deviation from stoichiometry Δs (Se-rich) remains nearly unchanged at Se vapor pressures higher than 1 Torr.
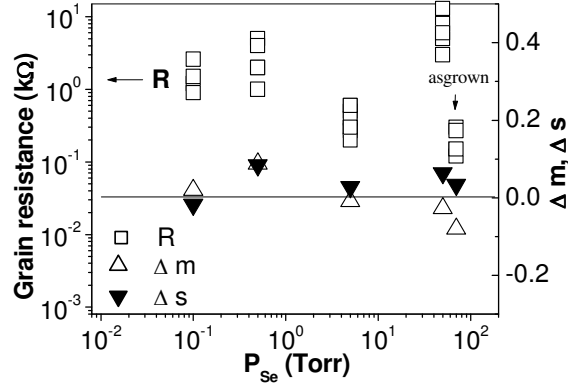
Fig. 3.12. Influence of Se vapour pressure on the CIS composition and grain resistance

The as-grown materials had lower resistivity than the selenium treated materials. We assume that selenium vapour pressure lower than 5 Torr did not hold back anymore the thermal dissociation of $CuInSe_2$ shown as the reaction (6):

$$2CuInSe_2 \rightarrow Cu_2Se(solid) + In_2Se(gas) + Se_2(gas); \qquad K_{CuInSe2} = P_{In2Se}P_{Se2}. \quad (6)$$
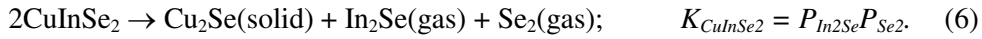
Higher selenium overpressures pushed the direction of this reaction to the left side. Fig. 3.13 shows the normalized photoluminescence (PL) spectra of CIS monograin powders heat-treated in Se vapors. It is seen that annealing in low-pressure selenium atmosphere (0.5 Torr) improves the crystallinity, as the signal/ noise ratio of the unishape spectrum is improved. Treatment at selenium pressure 50 Torr shifts the PL peak position to the higher value, up to 0.98 eV. This is attributed to the filling of Se vacancies in the process of high Se pressure annealing [41].
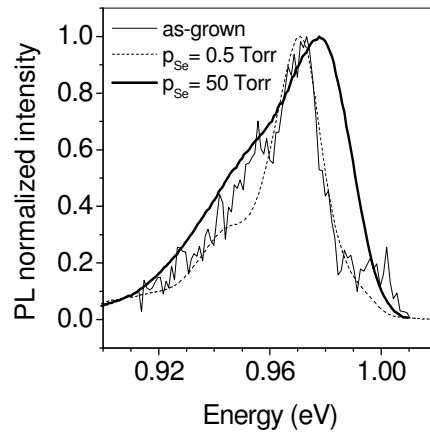
Fig. 3.13 PL spectra of nearly stoichiometric CuInSe₂
treated under different Se vapour pressure

32

Thermal treatment in sulphur vapour

Sulfurization of CIS is believed to be a promising method for absorber materials bandgap engineering. Furthermore, it has been reported that the incorporation of sulfur into CIS reduces the carrier recombination in the space charge region [85]. Sulfurization experiments were carried out in the same arrangement as selenization experiments.
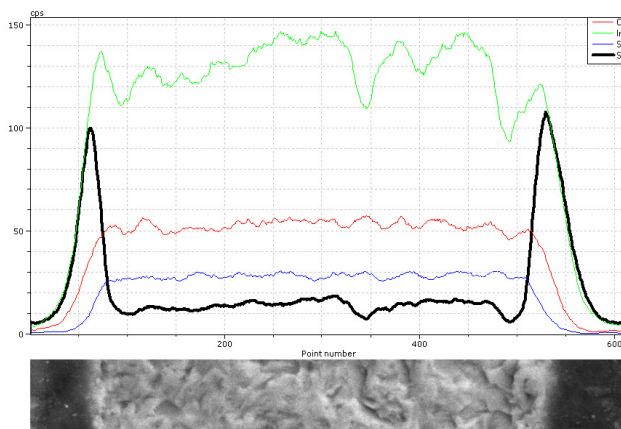
Fig. 3.14 EDX compositional profile of sulphur distribution

According to the XPS data, the surface composition of the sulfurized powder crystals was 8.5, 19.6, 15.3, and 56.6 mol % for Cu, In, S, and Se, respectively. This result shows that the surface composition of powder crystals is similar to the composition of $CuIn_3Se_5$ or a two-phase material containing $CuIn_3(Se,S)_5$ and $In_2(Se,S)_3$ [56]. At the same time, the bulk composition of the powder crystals corresponds to the $CuInSe_2$ compound: Cu, In, and Se contents in atom percentages were 23.8, 26.1, and 50.1, respectively (Cu/In=0.915).

Sulphur distribution in powder grains represents a gradient throughout the surface of grains to the volume. EDX compositional profile of sulphur distribution is given in Fig. 3.14.

Chemical etching of CuInSe₂ surface

The quality of interface between *p*- CuInSe$_2$ and *n*- CdS plays the key role in solar cell performance. Therefore, the quality of CIS grains surface cleaning and/or chemical etching before CdS deposition is very important. The effect of chemical treatment depends on concentration, temperature and chemical nature of etchant, sometimes also on the oxygen content in solution [69]. The chemical nature of etchant has a dramatic influence on both – on the surface composition and on the interface chemistry [49].

Etching of Cu-rich powders. In one of monograin layer solar cells technologies, the absorber crystals were embedded into polyurethane (PU). The contacting areas of crystals were released from PU by etching with KOH-EtOH. Polarographic analysis showed that the etching solutions of copper-rich (Cu:In:Se = 25,6 at.%:

24,2 at.%: 50,2 at.%) powders contained only selenium. Fig. 3.15 presents the surface of monograins after etching with KOH-EtOH solution.
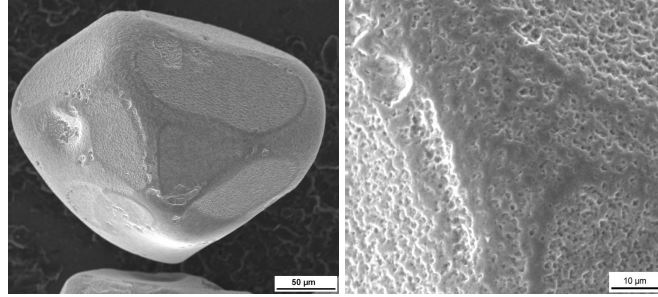
Fig 3.15. a) CIS monograin and b) grain surface after etching with KOH-EtOH solution

The removal process of the excess selenium from the material could be described as the following reaction:

$$3\ Se + 6\ KOH = K_2SeO_3 + 2\ K_2Se + 3H_2O \tag{7}$$
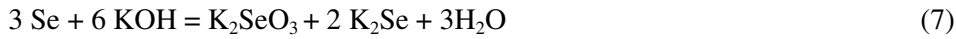
As a result, the crystal surfaces should remain metal-rich.
In order to eliminate semimetallic copper selenide phases and to improve the semiconductor behaviour of a Cu-rich CIS material, chemical etching of materials in KCN solution were performed.

$$2Cu(CN)_2 \rightarrow 2CuCN + (CN)_2 \tag{8}$$

$$CuCN \xrightarrow{\ CN^-\ } [Cu(CN)_2]^- \xrightarrow{\ CN^-\ } [Cu(CN)_3]^{2-} \xrightarrow{\ CN^-\ } [Cu(CN)_4]^{3-} \tag{9}$$

NH_3 solution is known as an effective solvent for the removal of surface oxides and the preferential etching of indium. The authors of [49,51] showed that NH_3 dissolves preferentially the In-rich, so-called ordered vacancy compound ($CuIn_3Se_5$) layer from the surface. On the base of XPS results they found that In-excess layer disappeared after 1-hour treatment in 1 M NH_3 aqueous solution at 60^oC, leaving behind the surface with nearly 1:1:2 composition. The behaviour of Cu-rich $CuInSe_2$ in ammonia solutions has not been studied yet. Our experiments showed copper and selenium concentrations (Cu/Se concentration ratio was between 1.4-2.4) higher than indium content in the leaching solutions of copper-rich monograin materials. The dissolution of copper from the material in aqueous ammonia solution could be described by the formation of soluble copper-ammonia complex ions ($[Cu(NH_3)_4]^{2+}$ and $[Cu(NH_3)_2]^+$):

$$Cu^{2+} + 4\ NH_3\ (aq) = [Cu(NH_3)_4]^{2+}\ (aq). \tag{10}$$

Kessler *et al.* [69] proposed that indium dissolution proceeds through the formation of oxides that are soluble in ammonia solution. A prerequisite for this is the

dissolved oxygen in the solution. Indium oxide is known as a native oxide on the CIS surface. Therefore, the oxidation-dissolution process should proceed on In-rich CuInSe$_2$ surface layers much faster than on Cu-rich layers. In monograin powders every grain is formed in the growth process as an individual micromonocrystal in isothermal equilibrium conditions by the liquid phase transport of the material. Thereby the homogeneity of the composition of CIS crystals in the whole powder is relatively high. This might be the reason for different results in our studies and presented in [69], where in the etching experiments of even slightly Cu-rich samples with NH$_3$ solution a relatively large loss of indium from materials was detected.

Etching of In-rich CuInSe$_2$ powders. The results of XPS analysis of chemically etched surfaces of In-rich CuInSe$_2$ powders are summarized in Table 3.2 and the results of the analyses of etching solutions in Table 3.3.

Table 3.2 XPS compositional analysis of chemically treated CIS powder surfaces

	Virgin surface composition (after S-treatment), at%	10% KOH-etOH 10 sec, at%	Conc. HCl 15 sec, at%	10% KCN 1min, at%
Cu	8.5	9.1	11.5	7.5
In	19.6	19.8	13.4	21.9
Se	56.6	54.3	59.1	53.7
S	15.3	16.8	16.0	16.9

These results show that the surface composition of powder crystals is similar to the OVC (ordered vacancy compound) or to a two-phase mixture of CuIn$_3$(Se,S)$_5$ and In$_2$(Se,S)$_3$ [56]. The bulk composition of In-rich powder crystals determined polarographically was: Cu 23.8 at%, In 26.1 at% and Se 50.1 at%.

Table 3.3 The concentration of elements in leaching solution as determined polarographically

	15 sec. HCl, mmole/ml	30 sec. KOH mmole/ml	1 min. KCN mmole/ml	15 min. NH$_3$ mmole/ml
Cu	no	1.3×10^{-5}	4×10^{-5}	6.8×10^{-5}
In	2.8×10^{-4}	2.2×10^{-5}	1.8×10^{-7}	3.8×10^{-5}
Se	no	1×10^{-5}	3.8×10^{-7}	No
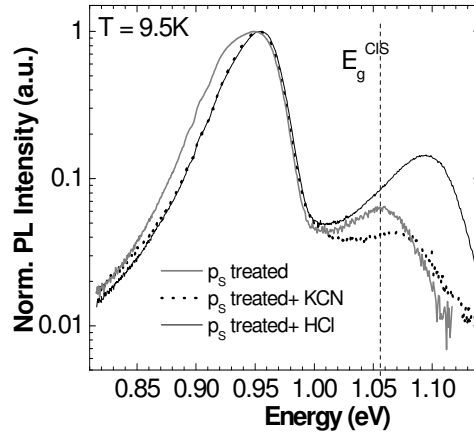
Fig. 3.16 PL spectra of the treated CuInSe₂ monograin powders

Fig. 3.16 shows the PL spectra of CIS powders after different chemical treatments. Two broad bands were detected in the measured PL spectra of CIS samples. The first asymmetric band with the maximum around 0.96 eV is typical of In-rich CIS [86]. The additional peak of PL emission at energies higher than the bandgap of stoichiometric CuInSe₂ (E_g=1.04 eV) indicates that there are other phases than 1:1:2 in our investigated CIS samples. We can expect that heat-treatment in sulphur vapour causes the formation of a solid solution on the surface. According to [87], this broad band with higher energy probably originates from $CuIn(S_xSe_{1-x})_2$ alloy. But it is also known that $CuIn_3Se_5$ and $Cu_2In_4Se_7$ phases have bandgaps higher than that of CuInSe₂ and usually show PL emission at $hv = 1.05 - 1.1$ eV [88,89]. Fig. 3.16 shows that HCl etching results in PL peak at higher energies, at $hv = 1.09$ eV. At the same time untreated and KCN treated powders indicate to the peak of PL emission at lower energies that could originate probably from the $CuIn_3Se_5$ separate phase in materials.

3.3. Solar cells based on CuInSe₂ monograin powder

The section describes the results of monograin layer technology development and characterization of the developed monograin layer solar cells. The current-voltage and quantum efficiency measurements give very important information about the properties of the developed photovoltaic devices. From the *I-V* measurements under illumination, solar cell parameters V_{oc}, *FF*, and J_{sc} were obtained.

36
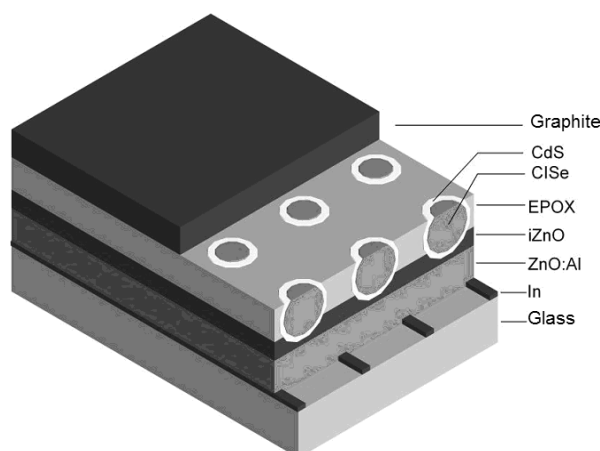
Fig. 3.17 Schematic illustration of the standard structure of CIS monograin layer solar cell

Fig. 3.17 shows the structure of the solar cells developed in the Laboratory of Semiconductor Materials. The "working" heterojunction is formed between the absorber and a *n*- type ZnO window layer. In order to improve the performance of the device, a thin, ~50 nm thick, CdS buffer layer is deposited between the absorber and window layers. The CdS buffer layer is structurally and electronically matched to the $CuInSe_2$ absorber and its presence decreases the density of interface states and prevents the inter-diffusion of components of absorber layer (i.e. Cu, In or Se) into the ZnO window layer, and vice versa. The CdS buffer layer is prepared by the chemical bath deposition (CBD) technique. ZnO is an ideal window material due to its wide bandgap (3.2 eV), high temperature stability and due to the fact that it can be doped in any desired order. The ZnO window layers are deposited by means of RF sputtering. The solar cell structure is completed by the evaporation of 1-2 µm thick indium grid contacts onto the ZnO window layer to diminish the loss of current carriers.

3.3.1.   Solar cells based on $CuInSe_2$ powders with different Cu/In ratio

As it was mentioned in the literature review, the performance of a solar cell is strongly influenced by the composition of the absorber layer and by the interface between the absorber layer and the following buffer layer.
Figs. 3.18a and 3.18b show the open circuit voltage (V_{oc}) and the short circuit current density (J_{sc}) of MGL solar cells depending on the Cu/In ratio of precursor Cu- In alloys. Dashed lines determine the concentration limits of the Cu-In alloy composition that allow the In-rich single phase $CuInSe_2$ absorber materials growth. Solar cells based on absorber layers prepared from slightly In- rich (Cu/In = 0.9) and stoichiometric (Cu/In = 1.0) CuIn alloys exhibited open circuit voltages up to 500mV and solar cell structure efficiencies up to ~ 9.5 %.
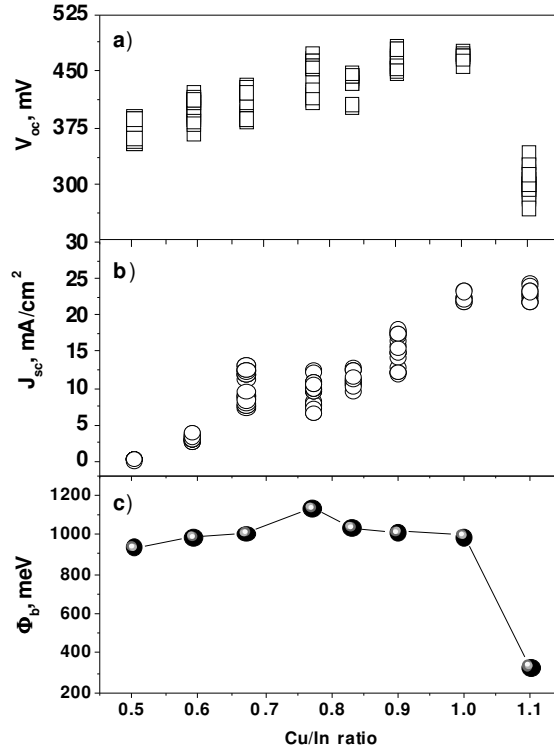
Fig. 3.18 a) Values of open circuit voltage (V_{oc}), b) values of current density (J_{sc}) and c) barrier height (Φ_b) of CIS MGL solar cells depending on different Cu/In ratios in the precursor CuIn alloy

The high In content (Cu/In<0.7) of the absorber material reduces the open circuit voltage and decreases the current density about 5 times. The completed cell structures from absorber materials with a substantial In-rich CIS composition (Cu/In<0.77), displayed non-ideal *S*-shaped *I-V* characteristics with fill factors (*FF*) less than 25% (Fig. 3.19). A sharp decrease in V_{oc} values was noticeable in the case of Cu-rich Cu-In precursor alloys (Cu/In=1.1) used.
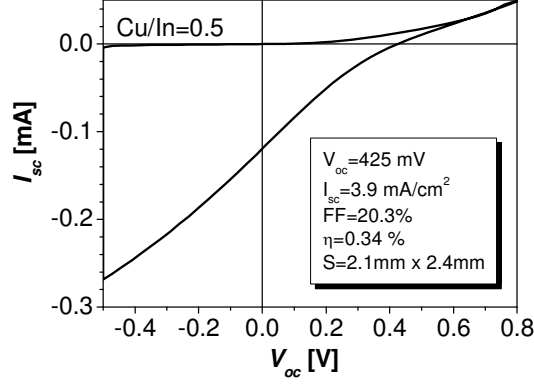
Fig. 3.19 *S*-shaped *I-V* curve for solar cells based on absorber with Cu/In ratio 0.5

The temperature dependent open circuit voltage measurements allow us to determine the barrier height of *p-n* junction (Φ_b) [90].

The open circuit voltage can be given by the following equation:

$$V_{oc} = \frac{\Phi_b}{q} - \frac{AkT}{q} ln\left(\frac{qS_p N_v}{j_{sc}}\right),$$ (1)

where *A* is the diode ideality factor, S_p is the interface recombination velocity, j_{sc} is the short circuit current density, *q* is the elementary charge, and N_v is the effective density of states in the valence band.

Dependence of Φ_b on the absorber layer composition is presented in Fig. 3.18c. The obtained barrier heights vary from 930–1140 meV. The barrier height depends on the Cu/In ratio because the S inclusion mechanism in CIS is a strong function of original composition of the absorber [43, 91]. The diffusion constants of sulphur in Cu-rich and In-rich materials are different by about two orders of magnitude. As a result, S inclusion is much more favourable in the Cu-rich material [43]. All the barrier heights are lower than the bandgap energy of $CuInS_2$ (E_g=1.5 eV) or the bandgap energy of the ordered vacancy chalcopyrite compound (OVC) ($E_g\approx$1.2eV). This is the evidence of interface recombination as the main recombination path for the photogenerated electrons [92].

The solar cell with absorber layer with Cu/In<0.77 has the highest barrier height of junction 1138±6 meV. Cu/In<0.77 represents the concentration region of Cu-In alloys, the conductivity type of absorber material changes from *p*- to *n*-type and the phase transition from chalcopyrite $CuInSe_2$ to $Cu_2In_4Se_7$ occurs. The existence of phase transition from chalcopyrite $CuInSe_2$ to $Cu_2In_4Se_7$ in this concentration area was experimentally verified by the hot probe and XRD measurements.

3.3.2. Solar cells based on post-treated CuInSe₂ powder materials

Solar cells based on vacuum annealed CIS absorber materials. The dependence of V_{oc} of solar cell structures that were made from vacuum annealed powders on the annealing time is presented in Fig. 3.20.
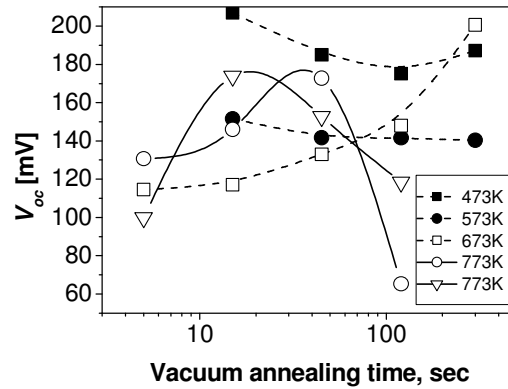
Fig. 3.20 V_{oc} **vs vacuum annealing time at different temperatures**

A short annealing duration at a low temperature, where the loss of selenium from absorber material prevails, results in a decrease of V_{oc}. At higher temperatures and for longer durations, the values of V_{oc} increase but remain relatively low. As a result, we can conclude that annealing in dynamic vacuum only does not allow us to obtain an absorber material with the composition necessary for high technical parameters of solar cells.
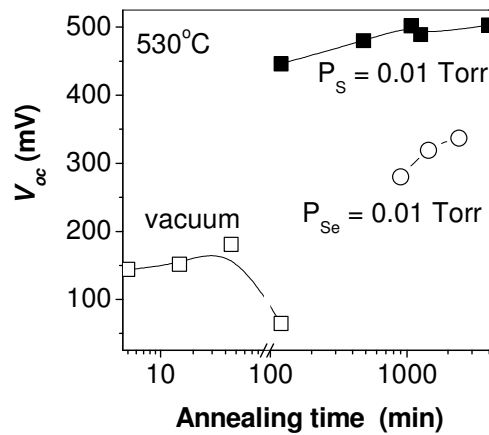
Fig. 3.21 Values of V_{oc} depending on the absorber material annealing time in different atmospheres

40

Solar cells based on selenisized CIS absorber materials. Heat treatments under Se vapor pressure was also performed at 803K for different durations for a material with the components ratio Cu/In=0.92. The use of powder annealed under Se vapor (0.01 Torr) for 40 h leads to the increase of open circuit voltage V_{oc} of the solar cell by up to 150 mV as compared to the cells in use of vacuum annealed materials (Fig. 3.21). At the same time, the values of the fill factor remained unchanged and had still low values.

Solar cells based on sulfurized CIS absorber materials. The efficiency of the CIS devices improved remarkably if CIS absorber material was additionally doped with sulfur. We found that an optimal annealing temperature for sulfurization is 803K. Fig. 3.22 shows the correlation between V_{oc} of the completed solar cells and the duration of material sulfurization. An increase in the annealing time resulted in a marginal increase in the V_{oc} values. However, sulphur incorporation consistently resulted in decreased short-circuit current (I_{sc}) values as compared with selenisized absorber materials.
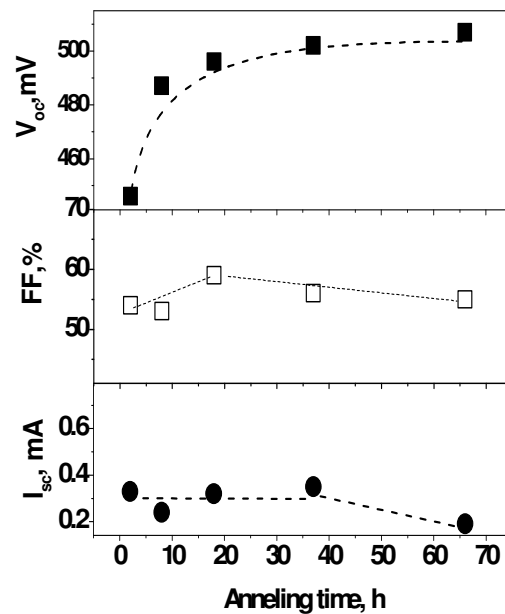
Fig. 3.22 Maximum output parameters of solar cells vs absorber material annealing time in sulphur vapour at 803K (p_S=0.01Torr)

Fig. 3.23 shows the dependence of the output parameters on the annealing temperature in sulphur vapour. After sulfurization, the efficiency of the active area of the cell improved drastically up to 9.5% with maximum V_{oc}=530mV, J_{sc}=25mA/cm^2 and FF=0.63, as compared to efficiencies before sulfurization. As

can be seen in Fig. 3.22, V_{oc} improved markedly and J_{sc} decreased, both of which can probably be attributed to an increase in the bandgap at the absorber surface due to the formation of a wider bandgap $CuIn(Se,S)_2$ layer. The improvement in V_{oc} is presumably due to the passivation of deep trap states, resulting in the lowering of space charge recombination [93,94], which also improved *FF*.
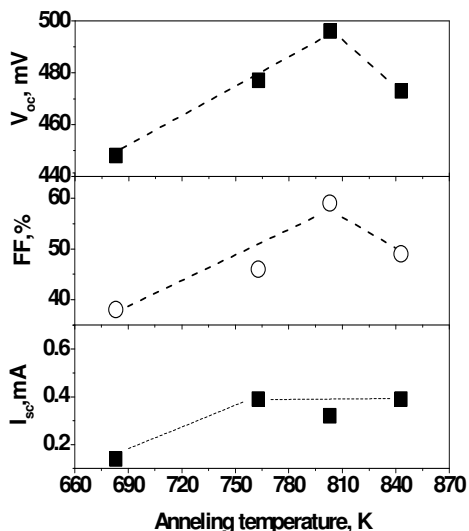
Fig. 3.23 Maximum output parameters of solar cells as a function of absorber material annealing temperature in sulphur vapour (p_S=0.01Torr, t=18h)

Solar cells based on chemically etched CIS absorber materials. All solar cells made from KOH-etched powders had the lowered values of open circuit voltages and short circuit currents as compared to those ones made from non-etched materials.
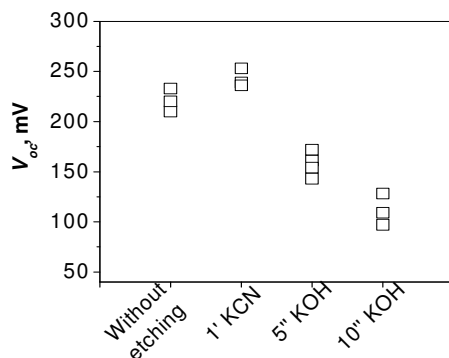
Fig. 3.24 V_{oc} of monograin layer CIS solar cells made from Cu-rich powders after etching in different etchants

Already 5-second etching of the material with KOH-EtOH decreased the value of V_{oc} more than 50 mV (see Fig. 3.24). Consequently, the removal of PU by KOH-EtOH etching is extremely critical for further success in monograin layer technology.

The KCN etching of Cu-rich monograin powders resulted in improved solar cell performance (see Fig. 3.24).

From the results of the present study, it can be concluded that the NH$_3$ treatment of Cu-rich CuInSe$_2$ absorber material depletes the surface from copper and selenium. As a result the open circuit voltage of solar cells decreased steadily with the variation of NH$_3$ etching time from 3 to 100 minutes (see Fig. 3.25).
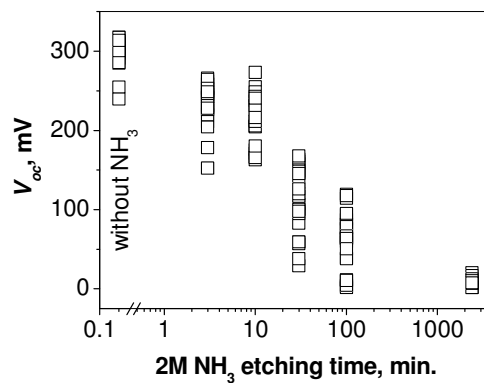
Fig. 3.25 Open circuit voltage (V_{oc}) as a function of NH$_3$ etching time

The results of *I-V* measurements of solar cells made from chemically treated In-rich materials are presented in Fig. 3.26. It can be seen that after KOH-EtOH treatment the values of I_{sc} are slightly lower, but the influence of etching is not so destructive as it was in the case of Cu-rich powders. In spite of this, our results
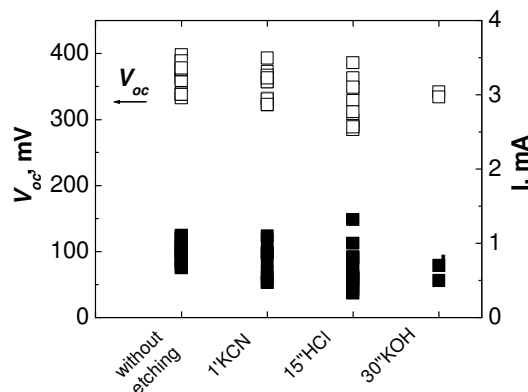
Fig. 3.26 V_{oc} and I_{sc} of solar cells made on the basis of chemically treated In-rich monograin powders

43

confirm that polyurethane-etching time with KOH-EtOH has a crucial influence to the parameters of the developed monograin layer solar cells.

The KCN etching is known as a process of removing binary phases of copper. Accordingly, treatment of In-rich powders with KCN should not have a substantial influence on the solar cell performance of the formed solar cell structures. Nevertheless, the KCN etching of our In-rich powders before CdS deposition resulted in improved fill factors and higher values of currents. The result could be explained by the removal of elemental S or Se extra phases in the KCN etching process. The formation of those extra phases on crystal surfaces after the Se or S vapour treatments is highly probable.

The other possible mechanism of the improvement of solar cell parameters is that the KCN etching depletes Cu sites on crystal surface, where later, in the process of CdS buffer layer deposition, Cd adsorption and diffusion occurs [95, 96, 97]. Cd atoms at Cu sites act as donor defects and, as a result, surface conductivity decreases and even surface conductivity conversion becomes possible [98,99]. Therefore, the interface recombination is decreased. The latter mechanism for solar cell improvement seems to be more likely, because the concentrations of removed Se and In in the leaching solution were found to be nearly two orders of magnitude lower than Cu concentration (see data in Table 3.1). Fig. 3.27 shows the current-voltage curves of the monograin layer solar cells used with materials with various KCN treatment durations.
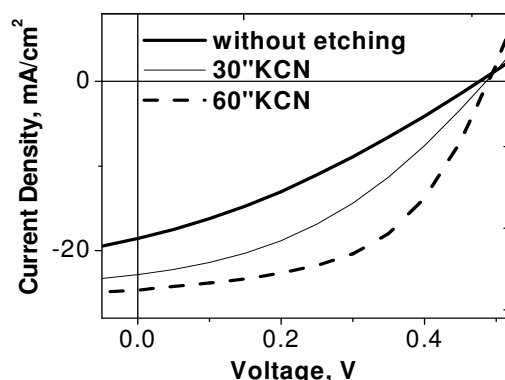
Fig. 3.27 *I-V* **curves of CIS solar cells with different KCN etching times**

HCl etching removes preferably indium from the CIS surface. The cells on the bases of HCl treated materials showed higher values of currents, but lower values of V_{oc} than the cells on the bases of untreated materials. As Cd atoms can reside on both Cu and In sites [99,100], then after HCl etching, Cd atoms can reside at removed In sites and act as acceptor defects, thus increasing surface conductivity.

Table 3.5 gives the maximum measured parameters of various CIS monograin layer solar cells prepared from various non-etched and etched materials.

Table 3.5 Performance characteristics of various CuInSe₂ monograin layer solar cells with and without etching

Etching time, etchant	V_{oc}, mV	J_{sc}, mA/cm^2	FF, %	η, %
Without etching	477	18.6	31.3	2.8
30 sec. KCN	486	22.9	39.0	4.3
1 min. KCN	489	24.7	52.6	6.3
5 sec. HCl	465	22.4	45.9	4.8
30 sec. HCl	477	24.8	46.7	5.5
1 min. HCl	473	24.8	51.8	5.9

In comparison with KCN etched samples, short time etching with concentrated HCl removes preferably In from the surface of the absorber material (Table 3.3) and leads to improved values of currents, but about 10 mV lower values of open circuit voltages (see Fig. 3.28).
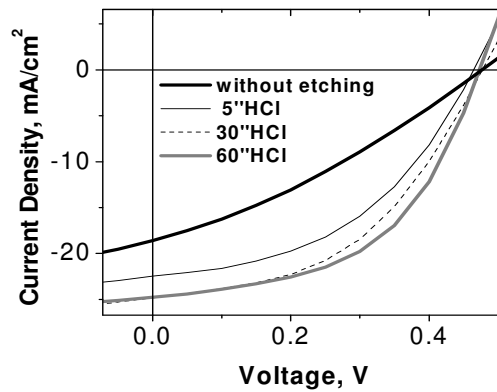
Fig. 3.28 *I-V* **curves of CIS solar cells with different HCl etching times**

3.4.   Quantum efficiency measurements

The quantum efficiency of solar cell structures was measured as a function of the wavelength of the incident light. Quantum efficiency is the measure of how efficiently a device converts the incoming photons to charge carriers.
Quantum efficiency measurements have been performed in order to compare the spectral response of the CuInSe₂-based solar cells with different solar cell performance. They reflect the charge carrier collection properties of the samples. The effective bandgap could be additionally estimated from the onset of charge collection at high wavelength. Fig. 3.29a shows the quantum efficiency (QE) versus the wavelength and Fig. 3.29b shows its first derivative versus energy for samples.
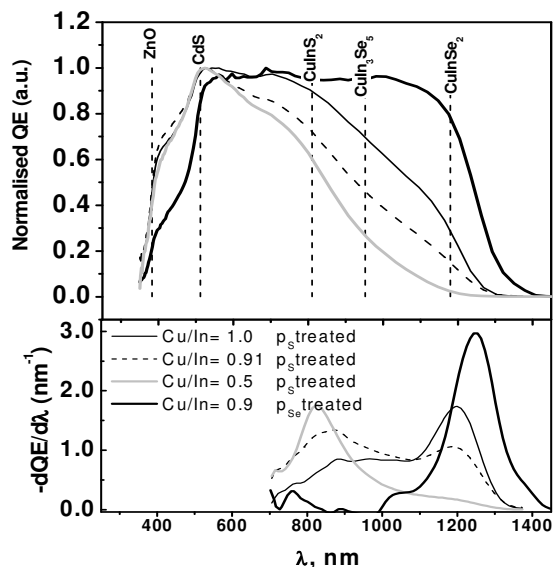
Fig. 3.29 a) The normalized quantum efficiency and b) derivatives of the QE spectra of MGL solar cell devices with different compositions of absorber material. Vertical bars indicate approximate positions of E_g of the components.

The behaviour of normalized quantum efficiency (QE) spectra of the solar cells depends drastically on the precursor composition and parameters of post-treatments (Fig. 3.29a). The only typical QE curve for pure $CuInSe_2$ was measured for the cell with the absorber layer of the powder (Cu/In = 0.9) and post-treated in selenium vapour. Significant loss in the long wavelength range of photons $\lambda > 800$ nm could be seen if MGL cells are made of sulphur vapour treated absorber layers. This loss indicates that carriers generated by long wavelength photons contribute to a smaller extent into the overall current.

The derivatives of quantum efficiencies (Fig. 3.29b) with respect to wavelength show two peaks at the energy values of ~1.4 eV and ~1.03 eV. The first peak is probably caused by the presence of a solid solution $CuIn_x(S, Se)_y$ phase formed in the near-surface region during the sulphurization process. The second peak position corresponds very closely to the bandgap energy of $CuInSe_2$. The first peak is the dominating one for the cells with the compositions in the range of 0.5<Cu/In<0.77. The second peak appears if the Cu/In ratio is between 0.8-1.0.

Bias-dependent external quantum efficiency measurements were performed for the investigation of carrier transport properties of devices of different absorber composition by applying reverse bias voltages of -2V and -3V (see Fig. 3.30). The figure shows typical behaviour of In-rich samples, where an applied bias leads to a significant change in quantum efficiency.

46
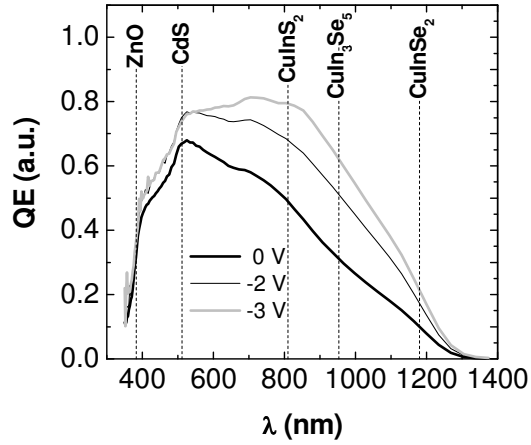
Fig. 3.30 Quantum efficiency measurements under 0V, -2V, -3V biases for In-rich solar cell devices

The relative change of quantum efficiency is wavelength-dependent and very pronounced in the near infrared light region. In brief, a large deviation of the stoichiometric composition results in changes of the electric properties and leads to the deterioration of photovoltaic performance, which mainly results in lower V_{oc} and *FF* values. A worsening of the solar cell parameters is accompanied by the reduction of the collection of charge carriers.

CONCLUSIONS

In the present thesis, the composition of CuInSe$_2$ powders grown in different molten fluxes with qualities acceptable for MGL design solar cells have been studied. The results show that the efficiency of the developed MGL solar cells is connected with bulk and surface composition of absorber materials.

Based on the results of chemical composition study of CuInSe$_2$ monograin powder, the following conclusions can be made:

- The composition of copper indium diselenide monograin powders depends on the origin of flux material.
    1. The composition CuInSe$_2$ monograin powders grown in the CuSe-Se flux is determined by the equilibrium of solid-liquid phases of CuInSe$_2$(solid)-CuSe-Se(liquid) at the growth temperature. In comparison with the phase equilibrium of CuInSe$_2$-Cu$_2$Se, the compositions of CuInSe$_2$ are shifted to more Cu-rich side. The shift depends on the Se content in liquid CuSe-Se flux. The powder crystals have p-type conductivity.
    2. Potassium iodide (KI) flux allows changing the composition of CuInSe$_2$ powders within a large deviation of molecularity. The conductivity type of as-grown crystals depends on the Cu/In ratio in the precursor Cu-In alloy. The existence range of single phase CuInSe$_2$ is between 0.77-1.0 of Cu/In ratio in the system CuInSe$_2$-KI at growth temperature 990K (versus 0.82-1.0 without KI).
    The optimal region of precursor CuIn alloy compositions for the growth of CuInSe$_2$ monograin powders as solar cell absorber materials in potassium iodide is between 0.9<Cu/In<1
- The heat treatment in vacuum yields in CuInSe$_2$ powders with Se-deficient composition and resistivity of material increases. Selenium vapour treatment modifies selenium concentration in CuInSe$_2$ powders depending on Se vapour pressure. Heat-treatment in sulphur vapour results in the formation of CuIn$_x$(Se,S)$_y$ solid solution on the crystal surface.
- The influence of chemical etchants on the CuInSe$_2$ surface composition depends on the deviations from the molecularity of absorber materials. The NH$_4$OH treatment of Cu-rich CuInSe$_2$ absorber material depletes its surface from copper and selenium. NH$_4$OH dissolves also indium from the In-rich CuInSe$_2$ absorber material. KCN removes preferentially copper and selenium from all CuInSe$_2$ absorber surfaces. HCl etching reduces the indium content in In-rich materials. KOH in ethanol etching removes selenium from the CuInSe$_2$ surface independent of the composition of the absorber.
- In a monograin layer solar cell the highest efficiency of ~9.5% is achieved using CuInSe$_2$ powders with Cu/In=0.92 grown in KI. The maximum output parameters for monograin layer solar cells are: V_{oc}=530mV, J_{sc}= 25 mA/cm^2 and FF= 63 %.

ACKNOWLEDGEMENTS

I would like to acknowledge efforts of each person who helped me carry the present thesis to a successful finish. I would also like to mention that the present work is not only the result of my research activities but it is rather a common effort of the monograin powder group at the Chair of Semiconductor Materials Technology.

First of all, I would like to express my deepest gratitude to my supervisor Mare Altosaar for her support, encouragement and advice during this work.

I would also like to thank Prof. Enn Mellikov, Head of the Department of Materials Science, for providing me the opportunity to join his group and to work in his laboratory.

I would like to thank Prof. Jüri Krustok for helpful discussions in the field of physics of solar cells.

This work would not have been possible without contribution and help from my colleagues from the Laboratory of Semiconductor Materials.
Special thanks are due to

- Jaan Raudoja and Kristi Timmo for help in sample preparation
- Tiit Varema, Kaia Ernits, Maris Pilvet for help in solar cell preparation
- Maarja Grossberg, Mati Danilson and Andri Jagomägi for help in optical measurements
- Olga Volobujeva for help in SEM and EDS measurements
- Malle Krunks for help in XRD measurements

I would also like to thank each colleague, former and present, at the Department of Materials Science, for pleasant working atmosphere and support and co-operation.

My warmest thanks belong to my family, especially to my son Mattias.

Tallinn, 2006

Marit Kauk

ABSTRACT

The main goal of the investigations this dissertation is based on was to find the regularities of formation and optimal composition of device-quality $CuInSe_2$ monograin powders for monograin layer solar cells.

The composition of $CuInSe_2$ as absorber materials in solar cells is a topic of main significance since the most important output parameters of solar cells are influenced by deviations from molecularity and stoichiometry. The bulk composition and the surface composition of CIS crystals can differ depending on deviations from molecularity and surface treatments. The doping of CIS with Na (K) also influences the surface composition and defect structure (electrical and optical properties). The growth of monograin powders proceeds in a flux material (CuSe, KI) at elevated temperatures, this enables us to dope the growing materials and has its peculiar impact on the properties of grown crystals.

This study focuses on the composition of $CuInSe_2$ monograin powders depending on the flux materials, variations of Cu/In in precursor alloys and post-treatments. Monograin powders were grown in CuSe-Se and KI as flux materials and Cu/In ratio varied from 0.5 to 1.1.

On the bases of the grown powders, the monograin layer solar cells were formed and investigated. A wide variety of characterization techniques was used to evaluate the material quality. The powders were characterized by polarographic analyses, EDS, SEM, XRD, photoluminescence spectroscopy and electrical properties by the hot-probe method. The monograin layer solar cells were examined by dark and light current-voltage (*I-V*) and quantum efficiency (QE) measurements.

It was found that the composition of $CuInSe_2$ monograin powders depends on the flux material. The use of CuSe-Se flux results in Cu-rich $CuInSe_2$ powders. The asgrown powder crystals have round shape and p-type conductivity with low electrical resistance. The KI flux allows growing In-rich $CuInSe_2$ powders. The conductivity type depends on the Cu/In ratio in the precursor Cu-In alloy. The crystals have tetragonal shape. The single phase CIS can be formed in the Cu/In ratio between 0.77-1.0.

Heat treatments in vacuum lead to $CuInSe_2$ powders with Se-deficient composition. Se vapour treatment increases Se concentration and resistivity is increased after selenization. According to the surface analysis, the sulphurization results in $CuIn(Se,S)_x$ solid solution on the crystal surface.

The influence of different etching procedures on the surface composition of CIS crystals was as follows: Cu-deficiency in the surface layer of CIS can be formed by KCN etching, In concentration can be reduced by HCl or NH_4OH etching and Se is removable by KCN and KOH etching.

The best CIS monograin layer solar cell have following output parameters:
V_{oc}=530mV, J_{sc}= 25 mA/cm^2, FF= 63% and efficiency of active area is ~9.5%.

KOKKUVÕTE
CuInSe$_2$ monoterapulbri koostise uurimine ja rakendus päikesepatareides.

Monoterapulber-tehnoloogia on suhteliselt lihtne, odav ja sobiv meetod pulbrilise absorbermaterjali valmistamiseks päikesepatareide jaoks. Tehnoloogia peamiseks eeliseks on see, et kristallide kasv sulandaja vedelfaasis tagab kristallide ühtlase koostise kogu pulbri mahus, mis on aluseks päikesepatareide reprodutseeritavatele omadustele.

Käesolevas töös uuriti CuInSe$_2$ monoterapulbrite koostise ja omaduste kujunemist kasvatamisel erinevates sulandates eesmärgiga kasutada neid monoterakiht-päikesepatareide absorberkihtide valmistamiseks. Absorbermaterjali koostise kõrvalekalle molekulaarsusest ja stöhhiomeetriast mõjutab nii materjali strukuuri, morfoloogiat kui ka elektrilisi ja optilisi omadusi.

CuInSe$_2$ monoterapulbrid kasvatati kasutades CuSe-Se ja KI sulandajat, mis põhjustab CuInSe$_2$ legeerimise oma- ja võõrlisanditega kasvuprotsessi käigus ja mõjutab kasvavate kristallide defektstruktuuri (elektrilisi ja optilisi omadusi) ja pinnakoostist.

Käesolavas töös uuriti CuInSe$_2$ monoterapulbri keemilist koostist, struktuuri, morfoloogiat sõltuvalt kasutatud sulandajast, Cu/In suhtest prekursorsulamis ja sõltuvalt järeltöötlustest, milleks olid termilised lõõmustused erinevates gaasikeskkondades ja keemilised absorbermaterjali pinnasöövitused.

Saadud materjalide omaduste iseloomustamiseks kasutati polarograafilist analüüsi, EDS, XRD, XPS, fotoluminessents spektroskoopiat ja elektriliste omaduste mõõtmist. Monoterapulbrite baasil formeeriti ZnO/CdS/CuInSe$_2$/grafiit stuktuuriga päikesepatareid, mille iseloomustamiseks kasutati volt-amper ja spekrtaal-tundlikkuse mõõtmisi.

Leiti, et CuInSe$_2$ monoterapulbri koostis sõtlub kasutatavast sulandajast.
CuSe-Se kasvatutud pulbrid saadi Cu-rikkad. Kristallid on ümarad, p-tüüpi juhtivuse ja madala takistusega. KI sulandajas kasvatatud pulbrid on In-rikkad. Kristallid on tetragonaalsed, juhtivustüüp sõltub Cu/In suhtest lähtesulamis. Päikesepatarei absorbermaterjaliks sobiva CuInSe$_2$ saadamiseks peab Cu/In suhe lähtesulamis olema vahemikus 0.77-1.0.
Järeltöötlus vaakumis muutis CuInSe$_2$ pulbri koostise Se-vaeseks. Seleniseerimine aitas tõsta Se sisaldust ja ühtlasi tõstis ka kristallide takistust. Väävi aururõhus töötlemine tekitas kristallide pinnale CuIn(Se,S)$_x$ tahke lahuse.

Keemilistest pinnatöötlustest selgus, et kasutatud söövituslahused omasid selektiivset söövitusvõimet: vase defitsiiti kristallide pinnakihis on võimalik saavutada söövitades KCN lahusega; In on võimalik eemaldada söövitades soolhappelise või ammoniakaalse lahusega; Se eemaldamiseks võib kasutada KCN või KOH lahuseid.

Parimate CuInSe$_2$ monoterakiht-päikesepatareide avatud pinna kasutegurid ulatuvad 9.5%, kusjuures V_{oc}= 530mV, J_{sc}= 25mA/cm2 ja FF= 63%.

Doktoritöö baseerub 10 artiklil, töö innovatiivsed tulemused on kaitstud 3 patendiga, millest kahes olen ka aurtoriks.

REFERENCES

1. A. Luque, S. Hegedus. 2003. Handbook of Photovoltaic Science and Engineering: Status, Trends, Challenges and the Bright Future of Solar Electricity from Photovoltaics, John Wiley & Sons, Ltd
2. S. Verma, N. Orbey, R. W. Birkmire, T. W. F. Russell, *Progress in Photovoltaics* 4 (1996) 341-353
3. V. Alberts, M. L. Chenene, *Phys. D: Appl. Phys.* 32 (1999) 3093–3098
4. H. Du, C.H. Champness, I. Shih, *Thin Solid Films* 480-481 (2005) 37-41
5. M.A. Contreras, B. Egaas, K. Ramanathan, J. Hiltner, A. Swartzlander, F. Hasoon, R. Noufi, *Prog. Photovolt.: Res. Appl.* **7** (1999), 311-
6. M. A. Contreras, M. J. Romero, R. Noufi, *Thin Solid Films* 511-512 (2006) 51-54
7. D. Meissner, E. Mellikov, M. Altosaar, Einkristallpulver- und Monokorn-membran- herstellung, Patent of Germany #19828310, 6.09.2000
8. M. L. Fearheiley, *Solar Cells* 16 (1986) 91-100
9. C.H.Champness, *Journal of Materials Science: Materials in Electronics* 10 (1999) 605-622
10. H. W. Spiess, U. Haeberlen, G. Brandt, A. Raeuber, and J. Schneider, *Phys. Status Solidi B* 62 (1974) 183 - 192
11. R. Diaz, J. M. Merino, M. Leon, J. L. Martin de Vidales, F. Rueda, *Jpn. J. Appl. Phys.* 39-1 (2000) 339-342
12. T. Gödecke, T. Haalboom, F. Ernst, *Zeitschrift für Metallkunde* 91 (2000) 622 - 634
13. U.- C. Boehnke, G. Kühn, *J. Mater. Sci.* 22 (1987) 1635 -
14. T. I. Koneshova, A.A. Babitsyna, V.T. Kalinnikov, *Izv. Akad. Nauk. SSSR Neorg. Mater.* 18 , No 9 (1982) 1483-1486
15. T. Haalboom, T. Gödecke, F. Ernst, M. Rühle, R. Herberholz, H. W. Schock, C. Berlharz, K. W.Berz, *Inst. Phys. Conf. ser. No 152: Section B: Thin Film Growth and Characterization* (1997) 249-252
16. C. Beilharz, K.W.Benz, I. Dirnstorfer, B.K.Meyer, *Ternary and Multinary Compounds : proceedings of the 11th International Conference on Ternary and Multinary Compounds (ICTMC-11)*, (1997) 19-22
17. U. Rau, H. W. Schock, *Applied Physics A* 49, (1999) 131-147
18. R. Herberholz, U. Rau, H. W. Schock, T. Haalboom, T. Gödecke, F. Ernst, C. Beilharz, K. W. Berz, D. Cahen, *Eur. Phys. J. AP* 6, (1999) 131-139
19. H. Neumann, *Sol. Energy Mater. Sol. Cells* 16 (1986) 317- 333
20. J. Parkes, R. D. Tomlinson, M. J. Hampshire, *J. Appl. Cryst.* 6 (1973) 414-416
21. J. L. Shay, B. Tell, H. M. Kasper, L. M. Schiavone, *Phys. Rev. B* 7 (1973) 4485–4490
22. L. L. Kazmerski, M. S. Ayyagari, F. R. White, G. A. Sanborn, *J. Vac. Sci. Technol.* 13 (1976) 139 -
23. J. A. Groenink, P. H. Janse, *Z. Phys. Chem. Neue Folge* 110 (1978) 17-28

24. R. Noufi, R. Axton, C. Herrington, S. K. Deb, *Appl. Phys. Lett.* 45 (1984), 668-670
25. R. H. Bube, Photovoltaic Materials, Imperial College Press, London, 1998
26. S. M. Firoz Hasan, M. A. Subhan, Kh. M. Mannan, *Optical Materials* 14 (2000) 329-336
27. S. B. Zhang, S. H. Wei, A. Zunger, *Phys. Rev. B* 57 (1998) 9642–9656
28. H. Y. Ueng, H. L. Hwang, *Mater. Sci. Eng. B* 12 (1992) 261–267
29. E. I. Rogacheva, *Inst. Phys. Conf. Ser.* 52 (1998) 1–14;
30. C. Rincon, R. Marquez, *J. Phys. Chem. Solids* 60 (1999) 1865–1873;
31. H. H. Chan, H. Y. Ueng, T. X. Zhong, H. L. Hwang, *Jpn. J. Appl.Phys.* 39 (2000) 399–401
32. E. I. Rogacheva and T. V. Tavrina, *Journal of Physics and Chemistry of Solids* 64, Issues 9- 10 (2003) 1911-1915
33. H. J. Von Bardeleben, *Solar Cells* 16 (1986) 381-390
34. K. Senthila, D. Nataraja, K. Prabakara, D. Mangalaraja, Sa. K. Narayandassa, N. Udhayakumarb, N. Krishnakumar, *Materials Chemistry and Physics* 58 (1999) 221-226
35. C. Guillen, J. Herrero, *Solar Energy Materials and Solar Cells* 43, (1996) 47-57
36. C. H. Champness, G. I. Ahmad, *Thin Solid Films* 361-362, (2000) 482-487
37. A. A. S. Akl, A. Ashour, A. A. Ramadan, K. Abd EL- Hady, *Vacuum* 61 (2001) 75- 84
38. V. Alberts, M. Klenk, A. Bucher, *Jpn. J. Appl. Phys.* 39 (2000) 5776- 5780
39. A. Ashour, A. A. S. Akl, A. A. Ramadan, K. Abd EL- Hady, *Thin Solid Films* 467 (2004) 300 – 307
40. J- F. Guillemoles, P. Cowache, A. Lusson, K. Fezzaa, F. Boisivon, J. Vedel D. Lincot, *J. Appl. Phys.* 79 *(9)* (1996) 7293-7302
41. V. Alberts, J. Bekker, M. J. Witcomb, J. H. Schön, E. Bucher, *Thin Solid Films* 361–362 (2000) 432–436
42. H. Neumann, R. D. Tomlinson, *Solar Cells* 28 (1990) 301-313
43. B. M. Basol, A. Halani, C. Leidholm, G. Norsworthy, V. K. Kapur, A. Swartzlander, R. Matson, *Prog. Photovolt. Res. Appl.* 8 (2000) 227-235
44. J. Titus, H. W. Schock, R. Birkmire, W. N. Shafarman, U. P. Singh, *Mat. Res. Soc. Symp. Proc.* Vol. 668 (2001)
45. V. Alberts, F. D. Dejene, *J. Phys. D: Appl. Phys.* 35 (2002) 2021-2025
46. T. Walter, R. Menner, C. Köble, H. W. Schock, *Proceedings of the 12th EC Photovoltaic Solar Energy Conference* (1994) 1755
47. S. Pecharrmant, J.- F. Guillemoles, J. Vedel, D. Lincot, J. M. Siffre, H. Ardelean, M. Marcus, *Ternary and Multinary Compounds : proceedings of the 11th International Conference on Ternary and Multinary Compounds* (ICTMC-11) (1997) 719-722
48. C. Hack, G. Müller, *Proceedings of 16th European Photovoltaic Solar Energy Conference,* Glasgow (2000)

49. T. Desol, M.C. Simmonds, I. M. Dharmadasa, *Sol. Energy Materials & Solar cells* 77 (2003) 331-339

50. R. Klenk, R. Menner, D. Cahen, H. W. Schock, *Proceedings of 21st IEEE Photovoltaic Specialists Conference* (1990) 481- 486

51. Y. Hashimoto, N. Kohara, T. Wada, T. Negami, M. Nishitani, *Jpn. J. Appl. Phys.* 35 (1996) 4760-4764

52. T. Wada, Y. Hashimoto, K. Kusao, N. Kohara, T. Negami, M. Nishitani, *Mat. Res. Soc. Symp. Proc.* Vol. 426 (1996) 291-296

53. U. Störkel, M. Aggour, M. Weber, R. Scheer, H. J. Lewerenz, *Thin Solid Films* 387 (2001) 182-184

54. A. Rockett, R. W. Birkmire, *J. Appl. Phys.* 70, Issue 7 (1991) R81-R97

55. R. Pal, K. K. Chattopadhyay, S. Chaudhuri, A. K. Pal, *Thin Solid Films* 254, (1995) 111-115

56. A. J. Nelson, C. R. Schwerdtfeger, G. C. Herdt, D. King, M. Contreras, K. Ramanathan, W. L. O'Brien*, J.Vac. Sci. Technol. A* 15 (1997) 2058-2062

57. B. Canava, J. Vigneron, A. Etcheberry, D. Guimard, J.F. Guillemoles, D. Lincot, S. Ould Saad Hamatly, Z. Djebbour, D. Mencaraglia, *Thin Solid Films* 403- 404 (2002) 425-431

58. R. Hunger, T. Schulmeyer, M. Lebedev, A.Klein, W. Jaegermann, R. Kniese, M. Powalla, K. Sakurai, S. Niki, *Proceedings of WCPSEC*, Osaka (2003)

59. T. Atsintseva, Diploma thesis, Tallinn, TTU (1994)

60. M. Altosaar, E. Mellikov, Jpn. J.Appl. Phys., 39 (2000), Suppl. 39-1, 65-66

61. M. Altosaar, E. Mellikov, D. Meissner, J. Hiie, T. Varema, *Mat. Res. Soc. Symp. Proc.* 426 (1996) 563-569

62. M. Altosaar, J. Hiie, E. Mellikov, J. Mädasson, *Crystal Res. Technol.* 31 (1996) 505-508

63. J. Hiie, M. Altosaar, E. Mellikov, D. Meissner, T. Brammer, *Proc. of 2nd World Conf. on Photovoltaic Solar Energy Conversion* (1998) 732-734

64. Z. A. Shukri, C. H. Champness, *Journal of Crystal Growth* 191 (1998) 97-107

65. Yi-Chia Chen, Chin C. Lee, *Thin Solid Films* 283 (1996) 243-246

66. M. Elding- Ponten, L. Stenberg, S. Lidin, *J. Alloys & Comp.* 261 (1997) 162-171

67. N. Orbey, G. A. Jones, R. W. Birkmire and T. W. Fraser Russell, *Journal of Phase Equilibria* 21- 6 (2000) 509-513

68. B. Canava, J. Vigneron, A. Etcheberry, J. F. Guillemoles, D. Lincot, *Applied Surface Science* 202 (2002) 8-14

69. T. K. Bandiopadhyay, S. B. Chakraborty, S. R. Chaudhuri, *Physica Status Solid A* 108 (2) (1988) 119-123

70. J. Kessler, K. O. Velthaus, M. Ruckh, R. Laichinger, H. W. Schock, D. Lincot, R. Ortega, J. Vedel, *Proceedings of the PVSEC-6*, New Delhi, India, (1992) 1005-1010

71. Y. Okano, T. Nakada, A. Kunioka, *Solar Energy Materials & Solar Cells* 50 (1998) 105-110

72. H. Okamoto, Desk Handbook: Phase Diagrams for Binary Alloys, published by ASM International (2000), 308

73. H.Miyake, H. Ohtake, K.Sugiyama, *Journal of Crystal Growth* 156 (1995) 404-409

74. G. Massé, K. Guenoun, K. Djessas, F. Guastavino, *Thin Solid Films* 293, Issues 1-2 (1997) 45-51

75. M. A. Contreras, B. Egaas, P. Dippo, J. Webb, J. Granata, K. Ramanathan, S. Asher, A. Swartzlander, R. Noufi, *Proceedings of 26th IEEE Photovoltaic Specialists Conference* (1997) 359- 362

76. S.-H. Wei, S.B .Zhang, A. Zunger *J. Appl. Phys.* 85 (1999) 7214-7218

77. A. Rockett, J. S. Britt, T. Gillespie, C. Marshall, M. M. Al Jassim, F. Hasoon, R. Matson, B. Basol, *Thin Solid Films* 372, Issues 1-2 (2000) 212-217

78. M. Kauk, K. Timmo, M.Altosaar, J. Raudoja, Abstract book: Conference on Knowledge- based materials and Technologies for Sustainable Chemistry, Tallinn, Estonia, (2005) 90

79. H. P. Wang, I. Shih, C. H. Champness *Thin Solid Films 387*, Issues 1-2 (2001) 60-62

80. F. O. Adurodija, J. Song, S. D. Kim, S. H. Kwon, S. K. Kim, K. H. Yoon, B. T. Ahn, *Thin Solid Films* 338 (1999) 13-19

81. M. V. Yakushev, A. V. Mudryi , V. F. Gremenok , E. P. Zaretskaya , V. B. Zalesski, Y. Feofanov, R. W. Martin*, Thin Solid Films* 451 –452 (2004) 133-136

82. A. Ashida, Y. Shigeno, M. Segawa, N. Yamamoto, T. Ito, Ternary and Multinary Compounds : proceedings of the 11th International Conference on Ternary and Multinary Compounds (ICTMC-11) (1997) 75-78

83. se treatment bulk composition

84. H. Neumann, G. Kühn, *J. Less-Common Metals* 155 (1989) 13–17

85. T. Nakada, H. Ohbo, T. Watanabe, H. Nakazawa, M. Matsui, A. Kunioka, *Solar Energy Materials & Solar Cells* 49 (1997) 285-290

86. 0.96eV PL in-rich

87. A. V. Mudryi, I. A. Victorov, V. F. Gremenok, A. I. Shakin, M. V. Yakushev*, Thin Solid Film* 431- 432 (2003) 197-199.

88. S. Shirakata, S. Chichibu, H. Miyake, S. Isomura, H. Nakanishi, and K. Sugijama, *Inst. Phys. Conf. Ser. No.* 152 (1998) 597- 600.

89. Y. Hwang, B. Tseng, *Inst. Phys. Conf. Ser.* No. 152 (1998) 309- 312.

90. M. Schmidt, D. Braunger, R. Schäffler, H. W. Schock, U. Rau, *Thin Solid Films 361-362* (2000) 283-287

91. A. Stavrides, C. Yapp, W. Shafarman, R. Aparicio, R. Opila, R. Birkmire, *Proceeding of 31st IEEE Photovoltaic Specialists Conference*, Florida, USA, (2005) 247- 250

92. J. Krustok, M. Danilson, A. Jagomägi, M. Grossberg, J. Raudoja, *Proc. of SPIE* Vol. 5946 (2005) 236-242

93. U. Rau, M. Schmitt, D. Hilburger, F. Engelhardt, O. Seifert, J. Parisi, W. Riedl, J. Rimmasch, F. Karg, *Proceeding of 25th IEEE Photovoltaic Specialists Conference,* Washington, (1996) 1005- 1008

94. D. Ohashi, T. Nakada, A. Kunioka, *Solar Energy Materials & Solar Cells* 67 (2001) 261-265

95. T. Wada, S. Hayashi, Y. Hasimoto, *Proc. 2nd World Conf. Photovoltaic Sol. Energy Conv.*, Vienna, (1998) 403-408

96. T. Nakada, *Thin Solid Films* 361-362 (2000) 346-352

97. D. Liao, A. Rockett, *J. Appl. Phys.* 93 (2003) 9380-9382

98. K. Ramanathan, F. S. Hasoon, S. Smith, D. L. Young, M. A. Contreras, P. K. Johnson, A. O. Pudov, J. R. Sites, *J.Phys. Chem. Sol* 64 (2003) 1495-1498

99. T. V. Tavrina, E. I. Rogacheva, *J. Phys. Chem. Sol* 64 (2003) 1917-1921

100. P. Fons, K. Sakurai, A. Yamada, K. Matsubara, K. Iwata, T. Baba, Y. Kimura, H. Nakanishi, S. Niki *J.Phys. Chem. Sol* 64 (2003) 1733-1735

APPENDIX A

Article I

M. Kauk, M. Altosaar, J. Raudoja, A. Jagomägi, M. Danilson, T. Varema, The performance of CuInSe$_2$ monograin layer solar cells with variable indium content, *accepted for publication in the Thin Solid Film, presented in the conference E-MRS 2006*

Appendix A

Article II

K.Timmo, M.Altosaar, **M.Kauk**, J.Raudoja, E.Mellikov, $CuInSe_2$ monograin growth in the liquid phase of potassium iodide, *accepted for publication in the Thin Solid Film, presented in the conference E-MRS 2006*

Appendix A

Article III

M.Kauk, K.Ernits, M. Grossberg, J.Krustok, T. Varema, M.Altosaar, E.Mellikov
Chemical etching of $CuInSe_2$ absorber surface for monograin layer solar cell
application, *Proceeding of 20th European Photovoltaic Solar Energy Conference
and Exhibition* (2006) 1811 – 1814

Appendix A

Article IV

M. Altosaar, M. Danilson, **M. Kauk**, J. Krustok, E. Mellikov, J. Raudoja, K. Timmo, T.Varema, Further developments in CIS monograin layer solar cells technology, *Solar Energy Materials & Solar Cells* 87 (2005) 25-32

Appendix A

Article V

M. Kauk, M. Altosaar, J. Raudoja, K. Timmo, M. Grossberg, T. Varema, E. Mellikov, Growth of CuInSe$_2$ monograin powders with different compositions, *Mater. Res. Soc. Symp. Proc.* Vol. 865, *Thin-Film Compound Semiconductor Photovoltaics*, 2005 F 14.27

Appendix A

Article VI

M.Kauk, M.Altosaar, J.Raudoja, K.Timmo, M. Grossberg, T.Varema, K.Ernits, Tailoring the composition and properties of CuInSe$_2$ materials for solar cells application, *Proc. SPIE Vol. 5946, Optical Materials and Applications*, 2005, 224-229

Appendix A

Article VII

M.Altosaar, A.Jagomägi, **M.Kauk**, M.Krunks, J.Krustok, E.Mellikov, J.Raudoja, T.Varema, Monograin layer solar cells. *Thin Solid Films* 431-432 (2003) 466-469

Appendix A

Article VIII

M.Kauk, M.Altosaar, J.Raudoja Influence of vacuum annealing on the composition of $CuInSe_2$, *Photovoltaic and Photoactive Materials - Properties, Technology and Applications, Kluwer academic publishers,* Vol. 80, (2002) 337-339

Appendix A

Article IX

M.Altosaar, **M.Kauk**, J.Raudoja, T.Varema, V.Geyer, Verfahren zur Behandlung von Pulverkörner, Application for European Patent, EP1548845, 29.06.2005

Appendix A

Article X

M.Altosaar, **M.Kauk**, J.Raudoja, T.Varema, V.Geyer, Method for treating powder particles, Application for International Patent, WO2005064691, 14.07.2005

Elulookirjeldus

Ees- ja perekonnanimi	Marit Kauk
Sünniaeg ja -koht	25.04.1977 Kohtla-Järve
Kontaktandmed	
Aadress	Vatsla 4/4, Saue vald, Harjumaa, 76902
Telefon	+372 55 688 092, 6203362 (tööl)
E-post	kmarit@staff.ttu.ee
Hariduskäik	1995 – Tabasalu Keskkool, keskharidus
	2000 – Tallinna Tehnikaülikool, keemia - ja materjalitehnoloogia teaduskond, loodusteaduste bakalaureuse kraad
	2002 – Tallinna Tehnikaülikool, keemia- ja materjalitehnoloogia teaduskond, loodusteaduste magistrikraad
Teenistuskäik	1999 - 2002 Tallinna Tehnikaülikool, Pooljuhtmaterjalide labor, insener
	2002 -…Tallinna Tehnikaülikool, Pooljuhtmaterjalide labor, teadur
	2004-… Tallinna Tehnikaülikool, Materjaliteaduse instituut, assistent
Kaitstud lõputööd	"I-III-VI$_2$ tüüpi ühendite keemilise koostise uurimine polarograafilisel meetodil", bakalaureusetöö, juhendaja vanemteadur Mare Altosaar
	"CuInSe$_2$ koostise uurimine", magistritöö, juhendaja vanemteadur Mare Altosaar
Täiendõpe	sept. 2001 "NATO ASI Photovoltaic and Photoactive Materials – Properties, Technology and Application", Sozopolis, Bulgaarias
	mai 2002 CEI-Europe Advanced Technology Education "Thin Film Deposition and Applications", Uppsalas, Rootsis
	okt. 2003- dets. 2003 täiendõpe Stuttgarti Ülikoolis, Saksamaal
	aug.-sept. 2005 täiendkoolitus Berliinis, Saksamaal
	aug. 2006 noorteadlaste suvekool "YSSS-2006 on PV" Valgerannas, Pärnumaal

Curriculum vitae

First name and surname	Marit Kauk
Date and place of birth	25.04.1977 Kohtla-Järve
Address	Vatsla 4/4, Saue vald, Harjumaa, 76902
Telefon	+372 55 688 092, 6203362
E-mail	kmarit@staff.ttu.ee
Education	1995 – Tabasalu Secondary School

2000 – Tallinn University of Technology, Faculty of Chemistry and Materials Technology, Bachelor of Science in Natural Sciences
2002 – Tallinn University of Technology, Faculty of Chemistry and Materials Technology, Master of Science in Natural Sciences

Professional experience

1999 - 2002 Tallinn University of Technology, Department of Materials Science, engineer
2002 -…Tallinn University of Technology, Department of Materials Science, researcher
2004-… Tallinn University of Technology, Department of Materials Science, assistant

Defended dissertations

"Study of I-III-VI$_2$ type materials composition by polarographic analysis", bachelor thesis, supervisor Senior Researcher Mare Altosaar
"Study of CuInSe$_2$ composition", master thesis, supervisor Senior Researcher Mare Altosaar

Training courses

Sept. 2001 "NATO ASI Photovoltaic and Photoactive Materials – Properties, Technology and Application", Sozopol, Bulgaria
May 2002 CEI-Europe Advanced Technology Education "Thin Film Deposition and Applications", Uppsala, Sweden
Oct. 2003- Dec. 2003 Stuttgart University, Germany
Aug.-Sept. 2005 PV Interact, Berlin, Germany
Aug. 2006 "Young Scientist Summer School on PV 2006" Valgeranna, Estonia